NTIS #PB2000-108445

SSC-413

EFFECT OF WELDED STIFFENERS ON CRACK GROWTH RATE

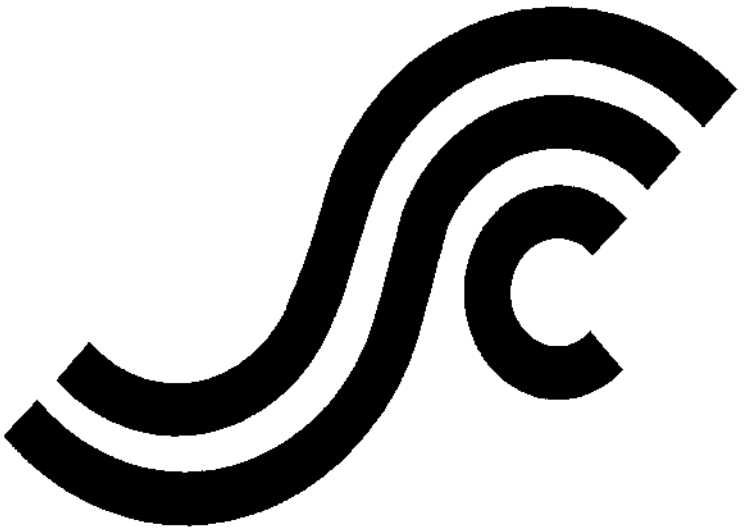

SHIP STRUCTURE COMMITTEE
2000

SHIP STRUCTURE COMMITTEE

RADM Robert C. North
U. S. Coast Guard Assistant Commandant,
Marine Safety and Environmental Protection
Chairman, Ship Structure Committee

Mr. Robert McCarthy
Director,
Survivability and Structural Integrity Group
Naval Sea Systems Command

Mr. Joseph Byrne
Director, Office of Ship Construction

Maritime Administration

Mr. Thomas Connors
Director of Engineering

Military Sealift Command

Dr. Donald Liu
Senior Vice President

American Bureau of Shipping

Mr. Bud Streeter
Director General, Marine Safety,
Safety & Security
Transport Canada

Dr. Neil Pegg
Group Leader - Structural Mechanics

Defence Research Establishment Atlantic

CONTRACTING OFFICER TECHNICAL REP.
Lieutenant David J. Martyn / Ms. Dinah Mulligan
U.S. Coast Guard R & D Center

EXECUTIVE DIRECTOR
Lieutenant David J. Martyn
U. S. Coast Guard

SHIP STRUCTURE SUB-COMMITTEE

AMERICAN BUREAU OF SHIPPING
Mr. Glenn Ashe
Mr. Yung Shin
Mr. Phil Rynn
Mr. William Hanzalek

MARITIME ADMINISTRATION
Mr. Chao Lin

NAVAL SEA SYSTEMS COMMAND
Mr. W. Thomas Packard
Mr. Edward E. Kadala
Mr. Allen H. Engle
Mr. Charles L. Null

UNITED STATES COAST GUARD
Captain Mark VanHaverbeke
Mr. Rubin Sheinberg
Mr. Walt Lincoln
Commander Ray Petow

DEFENCE RESEARCH ESTABLISHMENT ATLANTIC
Mr. Layton Gilroy
Mr. John Porter
LCDR Stephen Gibson
Dr David Stredulinsky

MILITARY SEALIFT COMMAND
Mr. Edward Meade
Mr. Rick A. Anderson
Mr. Jeffery E. Beach
Mr. Michael W. Touma

TRANSPORT CANADA
Mr. Nico Pau
Mr. James Reid

CANADIAN COAST GUARD
Mr. Justus Bunckhuysen

Member Agencies:

American Bureau of Shipping
Defence Research Establishment Atlantic
Maritime Administration
Military Sealift Command
Naval Sea Systems Command
Society of Naval Architects & Marine Engineers
Transport Canada
United States Coast Guard

Ship
Structure
Committee

An Interagency Advisory Committee

Address Correspondence to:

Executive Director
Ship Structure Committee
U.S. Coast Guard (G-MSE/SSC)
2100 Second Street, SW
Washington, D.C. 20593-0001
Ph: (202) 267-0003
Email: dmartyn@comdt.uscg.mil

SR-1392
SSC-413

September 2000

EFFECT OF WELDED STIFFENERS ON FATIGUE CRACK GROWTH RATE

The growth of large fatigue cracks was studied in welded, stiffened panels through the use of analytical, numerical and experimental means. Large-scale testing was conducted by intergrating welded, stiffened panels into a box girder configuration subjected to cyclic fatigue loading. The experiments show a decrease in the crack growth rate between stiffeners, which is attributed to compressive residual stress between stiffeners. Numerical modeling is performed using finite element models, with temperature gradients simulating residual stresses, to calculate the J-integral around the crack tip at different stages of crack development, and transforming the results into a propagation rate prediction. The two modeling techniques give similar results, validating the simpler analytical method. Either method can predict the results of the experiments conservatively with reasonable accuracy. Simple crack growth calculations, that ignore the residual stress fields and the stiffeners, give results that are too conservative by a factor of about three. On the other hand, simple correction factors for the stiffeners give very non-conservative results, also by a factor of about three.

R. C. NORTH
Rear Admiral, U. S. Coast Guard
Chairman, Ship Structure Committee

Technical Report Documentation Page

1. Report No. SSC-413	2. Government Accession No.	3. Recipient's Catalog No.
4. Title and Subtitle Effect of Welded Stiffeners on Fatigue Crack Growth Rate		5. Report Date **August 2000** 6. Performing Organization Code **Project No. 3301.03.05**
7. Author(s) **Robert J.Dexter and Paul J. Pilarski**		8. Performing Organization Report No. CG-D-05-00 SR-1392/R&DC-121-99
9. Performing Organization Name and Address University of Minnesota Dept. of Civil Engineering 122 CivE 500 Pillsbury Dr.S.E. Minneapolis, MN 55455-0116 U.S. Coast Guard Research & Development Center 1082 Shennecossett Road Groton, CT 06340-6096		10. Work Unit No. (TRAIS) 11. Contract or Grant No. DTCG -39-97-F-E00342
12. Sponsoring Agency Name and Address Ship Structure Committee C/O Commandant (G-MSE/SSC) United States Coast Guard 2100 Second Street, SW Washington, DC 20593-0001		13. Type of Report and Period Covered Final Report 14. Sponsoring Agency Code **G-M**

15. Supplementary Notes
Sponsored by the Ship Structure Committee and its member agencies

16. Abstract

The growth of large fatigue cracks was studied in welded, stiffened panels through the use of analytical, numerical, and experimental means. Large-scale testing was conducted by integrating welded, stiffened panels into a box girder configuration subjected to cyclic fatigue loading. The experiments show a decrease in the crack growth rate between stiffeners, which is attributed to compressive residual stress between stiffeners, case residual stress field representation. Numerical modeling is performed using finite element models, with temperature gradients simulating residual stresses, to calculate the J-Integral around the crack tip at different stages of crack development, and transforming the results into a propagation rate prediction. The two modeling techniques give similar results, validating the simpler analytical method. Either method can predict the results of the experiments conservatively with reasonable accuracy. Simple crack growth calculations that ignore the residual stress fields and the stiffeners give results that are too conservative by a factor of about three on the life. On the other hand, simple correction factors for the stiffeners give very unconservative results, also by a factor of about three.

17. Key Words	18. Distribution Statement
ship, fatigue, crack, stiffener, residual stress, fracture mechanics, finite element	Distribution Unlimited, Available From: National Technical Information Service U.S. Department of Commerce Springfield, VA 22151 Ph. (703) 605-6000

19. Security Classif. (of this report)	20. Security Classif. (of this page)	21. No. of Pages	22. Price
Unclassified	Unclassified		PC - MF -

ACKNOWLEDGMENTS

This research was conducted at the University of Minnesota under contract to J.J. McMullen Associates (JJMA). The study was funded by the United States Coast Guard Research and Development Center (USCGR&DC) at Groton Connecticut and was administered by the Ship Structure Committee. The authors are grateful for the support and for the guidance of the Project Technical Committee, particularly Robert Sedat of USCGR&DC. The patience and administrative support of Peter Fontneau at JJMA is also appreciated.

The authors are especially thankful for those who helped with the very difficult experimental work in the University of Minnesota's Structures Laboratory, particularly Paul Bergson. The development of the prediction models was greatly assisted by the advice of Alain Nussbaumer of EPFL Laussanne. Finite-element analyses were performed using ABAQUS at the Minnesota Supercomputing Institute (MSI). The authors appreciate the assistance of the staff at MSI as well as their generous donation of supercomputing resources to this project.

Executive Summary

Until recently, ship design practice was based primarily on yield and buckling considerations of structures subjected to maximum design loads. There was little explicit consideration of fatigue failure due to repeated lower level stresses caused by wave action, slamming and vibration. Some relatively new vessels, such as tankers in the TRANS Alaska Pipeline trade (TAPs), developed numerous small cracks. As long as these cracks remained small, they generally did not threaten the structural integrity of the ship. The high toughness of modern ship steels generally prevented sudden brittle fracture, so cracks could grow to considerable lengths before they posed serious structural problems. Nonetheless, cracking concerns did lead to increased requirements for inspection and repair, e.g., the Coast Guard requirements for Critical Area Inspection Plans (CAIPs). Much research was conducted to predict the initiation and development of such cracks, and classification societies' rules now require explicit consideration of fatigue failure.

Meanwhile, it is essential to be able to predict the safe service life of structures with various small cracks. Classical fracture mechanics offers methods to predict initiation and growth of fatigue cracks in homogenous plating. Real ship structures are complicated by the presence of stiffeners, and complex residual stress fields caused by welding of these stiffeners. The purpose of the current research is to assess methods to predict the growth of large cracks in realistic stiffened ship plating.

This report presents the results of a series of experiments with large cracks propagating across welded stiffened panels. Observed growth rates are compared to various predictive methods, from simple classical methods (modified to account for the presence of stiffeners and residual stresses), to detailed finite element methods executed on supercomputers. It is concluded that stable crack propagation behavior can be relied upon, and can be conservatively predicted using relatively simple approaches. These techniques can aid in making rational decisions regarding scheduling of repairs, and allow a better prediction of the risk to structural integrity from fatigue cracking.

TABLE OF CONTENTS

LIST OF FIGURES

LIST OF TABLES

LIST OF SYMBOLS AND ACRONYMS

α_1, α_2: Nussbaumer's coefficients used to correlate Isida's correction factor to that of the case with multiple stiffeners

β: Stiffener axial stiffness normalized to the projected stiffening area

Γ: Path of contour line

δ_c: crack tip opening value

δ_i: Residual stress at a given point

Δ: Change, Change in

$\Delta\sigma_{eff}$: Effective stress range

ΔK: Stress Intensity Factor Range

ΔK_{TH}: Threshold Stress Intensity Factor Range

$\Delta K_{applied}$, ΔK_{app}: Applied Stress Intensity Factor range (From external forces)

ΔK_{op}: Opening Stress Intensity Factor

ΔK_{total}: Stress Intensity Factor range for all acting force components

ΔK_{RP}: Stress Intensity Factor for the re-tensile plastic zone, (Toyasada et al, 157-58)

ΔK_{mc}: Stress Intensity Factor, crack in plate with multiple stiffeners, Petershagen and Fricke

η: Coefficient used in Faulkner's residual stress model

μ: Stiffness ratio of the stiffener to the plate

λ: Transverse stiffener spacing ratio

ρ: Required hole diameter to stop a propagating crack at a given ΔK

σ_0: Yield stress of plate material in Faulkner's residual stress model

σ_{nom}: Original stress on the original section

σ_{op}: Crack opening stress

σ_r: Magnitude of Faulkner's representative compressive stress block

$\sigma_{res}(x)$: Residual stress field

σ_y: Yield stress of the material

ξ: Rivet spacing ratio

χ: Ratio of crack distance to stiffener spacing

a: Half-crack length

a_{cr}: Critical crack length

a_i: Initial crack length

a_f: Final crack length

ABAQUS, ANSYS: Commercial FEA software package

ABS: American Bureau of Shipping

A_{pl}: Area of plate being stiffened

A_{st}: Area of stiffener

AISC: American Institute of Steel Construction

AWS: American Welding Society

B, b: Stiffener spacing

BS: British Standards (7608)

BSI: British Standards Institute

c: Distance of the crack tip from the stiffener centerline

c_0: Original centroid

c(a): Cracked section centroid

C: Experimentally determined coefficient used in the Paris Law

CAPS: Critical Area Inspection Plans

CCT: Center-Cracked Tension

C-Mn: Carbon-Manganese

CTOD: Crack Tip Opening Displacement

CVN: Charpy V-Notch

DnV: Det Norske Veritas, a classing society

E: Modulus of Elasticity

E_{pl}: Modulus of Elasticity for plate material

EPFM: Elastic-Plastic Fracture Mechanics

E_{st}: Modulus of Elasticity for stiffener material

f_σ: Net section coefficient, used as a finite width correction factor

f_1: Correction factor accounting for restraining effect of stiffeners, applied to the CCT K

f_2: Correction factor accounting for effect of severed stiffeners, applied to the CCT K

f_{Isida}: Correction factor, applied to K_{CCT}, to account for restraint of edge stiffeners

f_k: Koiter's finite width correction factor

f_s: Petershagen and Fricke correction factor to account for stiffeners, to be applied to K_{CCT}

f_{st}: Correction factor applied to K_{CCT} to account for effects of intact and severed stiffeners

f_w: Secant formula finite-width correction factor

FAD: Failure Analysis Diagram

FCAW: Flux-Core Arc Weld

F.E.: Finite Element

F.E.: Finite Element Analysis

FEM: Finite Element Model

F_i: Point force

HAZ: Heat-affected zone

I_0: Original moment of inertia

I(a): Cracked section moment of inertia

J: J-integral

k: Constant used in integrated form of the Paris Law

K: Stress Intensity Factor

K_1: Stress intensity factor for CCT plate

K_2: Stress intensity factor for plate without crack present

K_3: Stress intensity factor due to applied point forces

K_{IC}: Critical Stress Intensity Factor, Mode I (Opening crack)

K_C: Critical Stress Intensity Factor, general

K_{CCT}: Stress intensity factor for uniformly stressed plate with central notch

K_d: Dynamic Fracture Toughness

K_e: Effective Stress Intensity Factor

$K_{GREEN'S}$: Stress intensity factor due to pair of splitting forces

K_{RES}, K_r: Residual Stress Intensity Factor

$K_{res,\ gap}$: Residual Stress Intensity Factor, determined using F.E. analysis with gap elements

$K_{res,\ no\ gap}$: Residual Stress Intensity Factor, determined using F.E. with gap elements

K_{sp}: Stress intensity factor from superposition

K_{st}: Stiffened panel stress intensity factor

$K_{total, gap}$: Total Stress Intensity Factor, determined using F.E. analysis with gap elements

$K_{total, no\ gap}$: Total Stress Intensity Factor, determined using F.E. without gap elements

LEFM: Linear Elastic Fracture Mechanics

m: Material exponent used in the Paris Law

MSI: Minnesota Supercomputing Institute

N: Number of cycles

n_i: Number of stress ranges used in Paris Law summation

N_i: Number of cycles for a given stress range, used in Paris Law summation

NSWC: Naval Surface Warfare Center

$p_i(x)$: Pressure field

R: Load ratio

RF_{ms}: Reduction factor for multiple stiffeners

s: Half-stiffener spacing

S_i: Magnitude of stress in interval, used in Paris Law summation

S-N: Stress-Number of Cycles

S_r: Stress range

S_{Re}: Effective constant-amplitude stress range

SSC: Ship Structure Committee

t, t_{pl}: Plate thickness

T: Traction vector for evaluating contour integral

TAPS: Trans-Alaska Pipeline Service

U: Elber's Ratio (Proportion of effective stress)

V: Potential energy

W: Strain energy density

x: distance of point force from crack origin

INTRODUCTION

1.2 PROBLEM STATEMENT

Structural elements subjected to fluctuating loads of significant amplitude are susceptible to fatigue cracking [98, 33]. The primary variables influencing the possibility of fatigue cracking in welded steel structural elements are the severity of the stress concentration of the particular design detail and the nominal stress range, i.e. the algebraic difference between the maximum nominal stress and the minimum nominal stress. Ship structure is subjected to significant stress ranges from wave loading in rough seas as well as vibration from slamming or impact of waves, and therefore fatigue cracking is a potential problem with ships.

Classification societies have recently developed rigorous fatigue design criteria that should substantially reduce the incidence of fatigue cracking in ships [5, 30]. However, most ships in service today were not explicitly designed for fatigue, and consequently many of these ships are exhibiting frequent cracking [97, 2]. Fatigue cracking in modern ships is a serviceability problem rather than a structural integrity problem [118]. Fatigue cracks cause leaks and are a nuisance to repair. A large tanker may have hundreds or even thousands of fatigue cracks discovered during inspection [2, 97, 118, 149-151]. Yet these cracks are not an immediate threat to the structural integrity of the ship. The tolerance of ships to these cracks is attributable to the notch toughness of the steel and the overall structural redundancy.

Fatigue design is usually performed using the S-N approach, where structural details are grouped into categories sharing a common S-N curve. The S-N curve gives the number of cycles before the element develops a through-thickness crack, given the stress range for those N cycles. This approach is suitable for design. However, the number of cycles, S, to develop a through-thickness crack represents only a small fraction of the total fatigue life in redundant structures. In ships, cracks may propagate to lengths as great as eight meters before structural integrity is compromised.

Therefore, for assessment of existing ships and other structures, particularly if there are existing through-thickness cracks, a method is needed for predicting the safe propagation life of long, through-thickness cracks. The research involved in this report is focused on developing fatigue crack propagation models for predicting worst-case crack growth rates in welded stiffened panels, a common structural element in ship structure.

Although crack growth in plates and riveted stiffened panels (for airframes) has been studied extensively, few investigations of crack propagation in a panel with multiple welded stiffeners were found. Welded stiffeners affect crack growth in a unique way because of residual stresses present from the welding process. Furthermore, in contrast to riveted stiffeners, cracks may propagate into, and sever, integral welded stiffeners.

In addition to calculating the crack growth rate, it is also essential to determine a safe critical crack size. Current fracture models are based on brittle fracture and predict unreasonably conservative critical crack lengths on the order of 400-mm [129]. Field observations have consistently shown that crack lengths can greatly exceed the brittle fracture model predictions without a complete fracture occurring. For example, a crack 150-mm long was noticed in a U.S. Navy frigate and that this crack propagated to 8 meters in length during a severe 36-hour storm involving about 10,000 stress reversals. More recently, a 15-meter crack propagated across the deck of the 744-foot Ro-Ro (Roll-on, roll-off vehicle carrier) "Great Land" during a single severe storm without complete brittle fracture of the section [102]. Such tolerance illustrates the fracture resistance of typical ship steel and the need for improved models to take advantage of the residual strength found in the redundant structure.

Prior to 1940, steel ships were riveted. Riveted construction was good for structural integrity because a crack in one structural element could not propagate into adjoining structural elements. If a crack propagated in the shell, the intact structural elements, such as stiffeners, limited the crack opening and often arrested the crack growth. A corresponding increase in the amount of force carried by the stiffeners resulted from providing displacement control to the crack opening. This effect is known as load shedding.

During World War II, all-welded construction was introduced, perhaps most noted in the construction of Liberty Ships. A combination of steel with low notch toughness, poor weld processes, and high stress concentrating details contributed to brittle fracture in many of these ships [18]. In addition, welding creates tensile residual stresses near stiffeners, which tend to accelerate crack growth. The investigation of these fractures led to the founding of the Ship Structure Committee. These early investigations led to notch toughness requirements for ship steel, as well as improved welding methods and design details. The adoption of these provisions substantially reduced the incidence of brittle fracture.

The advent of high-strength steel in the 1970's allowed ship designers to design for a higher allowable stress. Unfortunately, the stress ranges increase in magnitude if the allowable stress is increased, because the scantlings are typically reduced relative to what they would be if low-strength steel were used. Although the yield and ultimate tensile strength of the steel had increased, the resistance to fatigue cracking of welded details is independent of the strength level and the type of steel [33, 34, 98, 52, 54, 69, 70]. Therefore, the higher stress ranges have translated to an increase in the incidence of cracking. Fortunately, the notch toughness of the steel and weld metal allows the cracks to grow in a stable manner.

The number of cracks observed in tankships has markedly increased in recent years, including those of the Trans-Alaska Pipeline Service (TAPS) [97]. As a result, frequent visual inspections are essential. A formal documentation plan known as NVIC 15-91 has been prepared by the U.S. Coast Guard regarding the tracking of various structural failures [163]. The guidelines describe three categories of "failures" that are related to the impact the failures could have on service structural performance. Ship owners submit the documentation, known as critical area inspection plans (CAIP's), as a method of monitoring the performance of repairs and a means of identifying areas of recurring failure.

Inspection procedures have been the subject of numerous investigations in terms of their quality and reliability as a fracture control procedure. A study by Kim et al. [84] concluded that cracks greater

than 200 mm in length could be detected 70% of the time, while a study by Demsetz estimated only a 50% probability of detecting a crack less than 300-mm [32]. These reports, in combination with the number of cracks surfacing in the aging tankships, has stimulated interest in understanding the behavior of cracks propagating through welded, stiffened panels.

There is a need to estimate the time before any crack can grow to a critical length, or length at which the ship's integrity is susceptible. Such estimates severely affect the profitability of ship transport, as any time out of service represents a substantial loss in revenue. At the same time, any risk of failure is a financial gamble as well. Better prediction models developed in this research will advance the assessment of safety and economic considerations.

1.3 OBJECTIVES OF THE PRESENT RESEARCH

One of the primary goals of this research is to recreate and observe fatigue crack propagation in a panel with multiple, welded stiffeners. Although fatigue cracks have been observed in the field, never before has load-controlled fatigue crack growth been recorded through multiple welded stiffeners.

The second objective is to investigate the load shedding effects of crack propagation through stiffening elements. The experimental setup attempts to simulate the cellular, redundant structure of tanker vessels. The growth of long fatigue cracks in a redundant system will allow observation of the interplay between crack growth parameters and structural performance.

A third objective is to gauge the significance of residual stresses on the rate of crack growth. Welding creates tensile residual stresses, on the order of the yield stress of the steel in the vicinity of the stiffeners, and lower level compressive stresses in the plating between the stiffeners. These stresses increase crack growth rates near stiffeners, and decrease (or arrest) it between stiffeners. It

is necessary to identify worst-case scenarios for crack growth rates to correctly estimate the time for a crack to propagate from the detectable size to the critical length.

Developing both analytical and finite element methods of predicting crack growth is the final goal of the research. These models of crack growth will facilitate successful use of these research results in the industry. Worst-case models of crack growth rates are compared with experimental results, bridging the gap between predictions and actual behavior. These models provide essential tools for fatigue life predictions, inspection interval rationale, and fitness for service qualifications for vessels containing the particular configurations tested.

1.4 FRACTURE MECHANICS

Fundamental principles of fracture mechanics are used to predict fatigue crack propagation. Linear Elastic Fracture Mechanics (LEFM) can be used under conditions where there is relatively little plastic deformation around the crack tip. LEFM is applicable to high-cycle fatigue crack growth, which typically occurs when applied stresses are well below the yield stress of the steel. LEFM is also usually applicable to brittle fracture, which often occurs at applied stress levels less than the yield stress.

Elastic-Plastic Fracture Mechanics (EPFM) considers limited amounts of plastic deformation during fracture. Both fields of Fracture Mechanics deal with fracture as a function of crack size, applied stress or displacement, and material toughness. There are many available texts that review the principles of both LEFM and EPFM [6, 15, 22]. Reemsnyder presented a review of fatigue and fracture principles relevant to ship structures [126]. The application of ductile fracture models is explained in a recent Ship Structure Committee report SSC-393 [35]. Therefore, only a brief review will be presented here.

The root of LEFM is the stress-intensity factor, K, which describes the magnitude of the stress field at the crack tip by relating it to the applied gross-section stress acting remotely from the crack plane and the crack length. The stress-intensity factor has units of MPa-$m^{1/2}$ in S.I. units and ksi-$in^{1/2}$ in English units, although ASTM has recently changed the English unit to the *Irwin*. Solutions have been obtained for the stress-intensity factor for various geometrical configurations and loadings, many of which can be found in handbooks [104, 131, 145]. Alternately, the stress intensity factor can be determined from finite-element analysis or other numerical methods.

The solution for the stress-intensity factor for a through-thickness crack in an infinite panel with an applied tensile stress is discussed here for example. The through thickness crack in an infinite plate

is also referred to as the center-cracked tension (CCT) panel. This solution forms the basis for most crack models for stiffened panels.

The relation is:

$$K = s\sqrt{p\,a} \qquad \text{Eqn. 0-1}$$

where "s" is the remotely applied nominal stress and "a" is the crack half-length, as described in Figure 2-1. The tensile stress should be taken as the stress in the panel at a distance away from the crack where the stress distribution appears uniform.

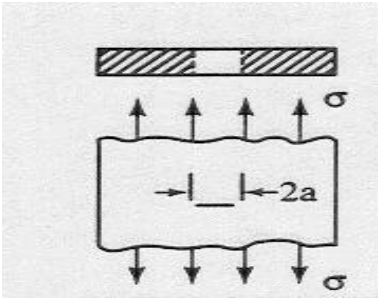

Figure 2-1: Through thickness crack in infinite plate under tension.

To predict the onset of fracture using LEFM, the material's fracture toughness is measured in terms of a critical stress-intensity factor, K_{Ic}. K_{Ic} may vary with constraint, loading rate, and temperature. In order to maintain linear elastic conditions, K_{Ic} must be measured with very large thick specimens to get valid results. For relatively thin plates (< 26 mm), it is impossible to get valid K_{Ic} values. Therefore, the fracture toughness is often estimated from correlation to "notch toughness", i.e. the results of the inexpensive Charpy V-Notch test (CVN) [22].

For ship structures, the loading rate is usually moderate and an appropriate K_c correlation to the CVN test is made by:

1) Obtain dynamic fracture toughness K_d from CVN through the relation:

$$K_d = 11.5\sqrt{CVN} \qquad \text{Eqn. 0-2}$$

where CVN is in Joules and K_d in MPa-$m^{1/2}$

2) Shifting the K_d curve -38 degrees Celsius to obtain an estimate of the fracture toughness appropriate for intermediate loading rates.

When linear elastic conditions exist, or in cases where plasticity around the crack tip is negligible, Linear Elastic Fracture Mechanics (LEFM) may be applied. As previously introduced (Eqn. 2-1), the K-factor characterizes the crack driving force. When plasticity effects are more substantial, the driving force may be characterized through the use of Elastic-Plastic Fracture Mechanics (EPFM). EPFM characterizes crack tip stress and strain fields through the use of the J-Integral or the Crack-Tip Opening Displacement (CTOD) rather than the stress-intensity factor. The J Integral is a measure of the change in potential energy associated with an incremental crack extension. It is usually calculated with a finite element analysis.

For linear elastic conditions, the J integral can be directly related to K. For plane-stress conditions:

$K = \sqrt{JE}$ where E is the modulus of elasticity. Eqn. 0-3

The crack-tip opening displacement (CTOD) is directly proportional to the J integral and therefore is really no different. However, the CTOD is the preferred EPFM parameter in some industries [33, 129].

To predict the onset of fracture in EPFM, the material's fracture toughness is measured in terms of a critical value of the J-integral or CTOD. Similar to K_c, the critical J or CTOD may vary with constraint, loading rate, and temperature. However, the requirements for specimen size and thickness are not nearly as stringent using these EPFM parameters.

The applied J-integral is often calculated using finite-element analysis. Dexter and Xiao [169] discussed issues involved in calculating J-integral values for stiffened panels in typical ship structure. These issues are also discussed in SSC-393 [35]. A comparison with the methodology and full-scale testing of structural components is made, and observations in J-integral behavior have led to a simple bi-linear approximation equation for applied J-integrals in assessing ductile fracture. Stenseng has also shown the use of this procedure applied to a plate with a single, coped stiffener and a crack emerging underneath [141].

EPFM is really only valid for limited amounts of plasticity. As explained in SSC-393 [35], the conditions of fracture in typical relatively thin (less than 26 mm thick) ship plate with notch toughness (CVN test) requirements involve extensive plasticity. This extensive plasticity invalidates the EPFM procedures. SSC-393 concludes that maximum load capacity of a cracked section in such relatively thin notch tough plate can be predicted accurately in terms of the plastic limit load for the net section.

The failure analysis diagram (FAD) is a convenient way of representing the interaction between fracture and net-section collapse. FADs are explained in detail in the paper by Reemsnyder [126] and in SSC-393 [35]. The FAD is also the basis of the procedures in PD-6493 [23]. PD6493 has very well documented step-by-step procedures for assessing fatigue crack growth and fracture from weld flaws. SSC-393 discusses ways that PD-6493 can be applied to larger cracks typical in ship structure.

Just as the range in stress governs the fatigue life of details, fatigue crack growth is governed by the range in stress-intensity factor, or ΔK. Paris noted that the rate of crack growth could be described by fitting a power law, which is known as the Paris Law [117].

The Paris law is expressed as:

$$\frac{da}{dN} = C * (\Delta K)^m \qquad \text{Eqn. 0-4}$$

where a = half crack length

N = number of cycles

C = an experimentally determined coefficient

ΔK = stress intensity factor range

m = material constant

The Paris Law is a relatively simple model that has proven to predict crack growth in a variety of situations with good success. Experimentally determined da/dN verses ΔK data typically exhibit a sigmoidal shape as shown in Figure 2-2.

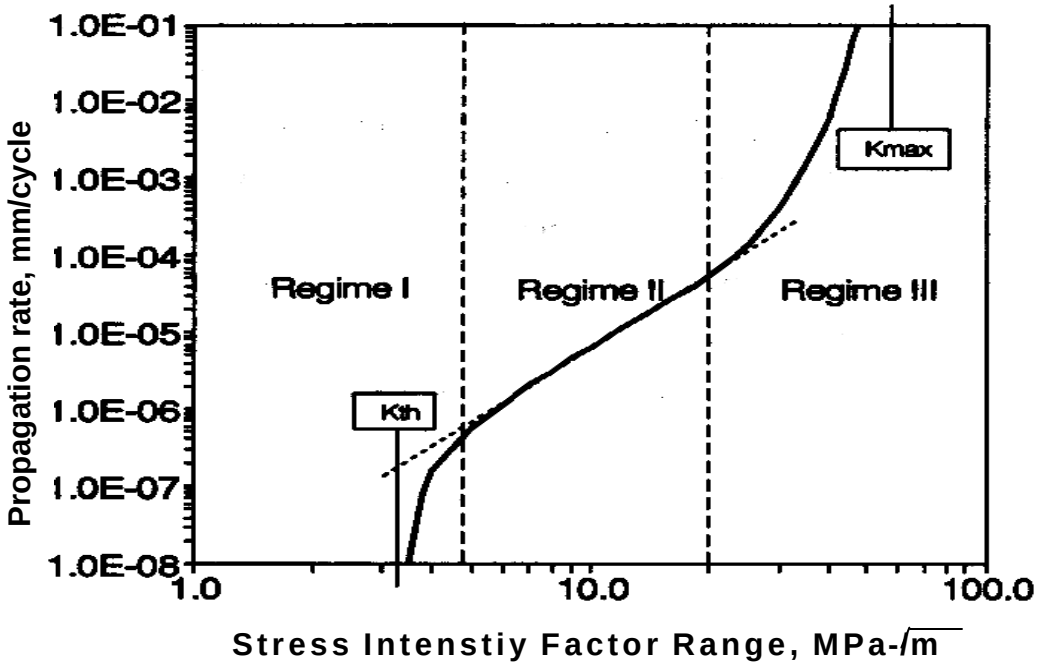

Figure 0-2: Typical plot of fatigue life [109].

The Paris Law is fit to the middle range of ΔK, from 5-20 MPa-$m^{1/2}$. Regime 1 indicates that there is a ΔK threshold, ΔK_{th}. For steel, the threshold value of ΔK is can be conservatively taken as 3 MPa-$m^{1/2}$. For values of ΔK greater than this threshold, fatigue crack growth obeys the Paris Law. Region 3 shows an acceleration of crack growth rate as ΔK approaches fracture toughness, K_{IC}. In

region 3 fatigue crack growth is accompanied by some ductile tearing or brittle fracture in each cycle.

It is important to keep in mind that it is difficult to achieve great accuracy using fracture mechanics to predict crack growth rate. First of all, there is a factor of ten or more scatter in experimental da/dN data. It is believed that a great deal of the scatter is due to experimental error, especially at low growth rates near the threshold because it is difficult to avoid the effect of prior precracking of the specimens at higher ΔK growth rates. (Unfortunately, this uncertain region at the low growth rates is also the most important for predictions, since most of the life is spent at these low growth rates.) However, there is believed to be a great deal of inherent variability in the actual growth rates, even if they were accurately measured.

To put the level of expected accuracy in perspective; one study [53] examined a large sample of fatigue tests where the welding defects causing the cracks was determined after the test from the fracture surfaces. One group of experiments involved continuous longitudinal fillet welds and another involved transverse groove welds. The fatigue lives were known and were also calculated using fracture mechanics. These are the best of conditions for a fracture mechanics calculation, where the stress and the defect size are known precisely.

The actual fatigue life was compared to the calculated fatigue lives. Various crack models gave a similar wide scatterband. The width of the scatterband was typically equal to a factor of three on life. When the same data are plotted in the S-N curve format, the scatter is on the order of a factor of ten on life. Therefore, it can be concluded that about 70 percent of the scatter in the S-N data are due to the effect of discontinuity size. However, the inherent variability of the growth rates undoubtedly contributes to the considerable remaining scatter.

The environment also influences crack propagation rates. The effects of seawater on crack growth in steel have been reported in SSC-326 and SSC-335 [25, 37]. A saltwater environment increases crack growth rates at higher ΔK ranges. In contrast, crack growth occurring in the near-threshold region exhibits decreased propagation rates. Such a phenomenon is explained by the corrosive

effects of saltwater—at low stress intensity factor ranges, corrosion product building up at the crack tip may actually retard crack growth by increasing crack closure. As the stress intensity factor range increases, however, corrosion product is less likely to cyclically accumulate at the crack tip, and instead corrosion assists crack growth. The environmental effects can often be included in the Paris Law by slightly changing the coefficients C and m.

The value of m, the exponent in the Paris Law, is typically is equal to 3.0 for steel in air. Careful experimentation shows this value of m to range from 2.8 to 3.2. As with any statistical fit to experimental data, misleading results can sometimes be obtained. Values of m as low as 2 and as high as 5 have been reported in the literature. However, it is our opinion, and the opinion of most other researchers working in fatigue, that the value of m should be 3.0, and the other reported values are actually due to error rather than actual variance in the slope of the data on the log-log plot.

Variance in the crack growth rate is usually expressed by variance in the coefficient C. Most researchers agree that all C-Mn steel has similar crack growth rates, and that the variance observed is just the typical material variation. In other words, there is not a real difference in the crack growth rates among various types of C-Mn steels, there is only scatter. As mentioned previously, the scatter can be substantial, on the order of a factor of 10 difference between the minimum crack growth rates and the maximum crack growth rates. Therefore, most reported values of C are intended to represent a conservative upper bound to the data.

Barsom and Rolfe [15] established an upper bound for a variety of ferritic steels where C was 6.8×10^{-12} for units of MPa and meters. However, the British Standard Institute PD6493 [31] recommend an upper bound of 9.5×10^{-12} for C. (Both of these sources agree that m is equal to 3 for steel). A recent study of HSLA-80 steel [53] showed that the upper bound crack growth rate was close to 9.0×10^{-12}, which is close to the upper bound recommended by PD6493. Therefore, it appears Barsom and Rolfe's upper bound is not sufficiently conservative.

Taking the slope m equal to 3, the Paris Law may be integrated to get an expression for N as a function of S_r and a:

$$N = \frac{k}{S_r^3}\left(\frac{1}{\sqrt{a_i}} - \frac{1}{\sqrt{a_f}}\right) \qquad \text{Eqn. 0-5}$$

where k is a constant, S_r is the stress range, and a_i and a_f are the initial and final crack length, respectively. The constant k is equal to $2/(C\pi^{1.5})$.

Figure 0-3 illustrates a typical S-N curve. The S-N curve is a design curve for characterizing the susceptibility of specific structural details to fatigue.

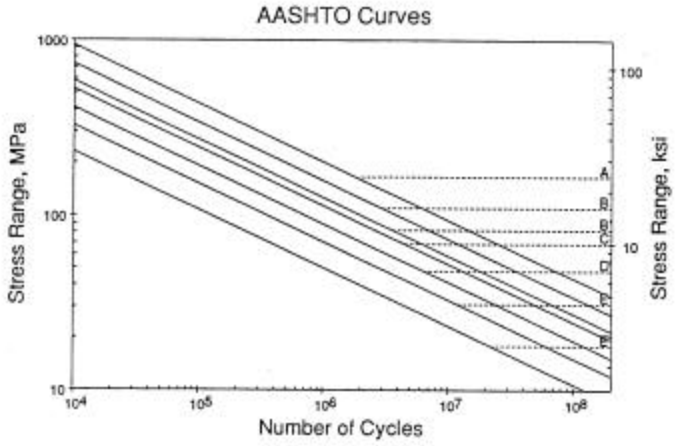

Figure 0-3: Typical S-N curve for fatigue design.

The integrated form of the Paris Law has the same form as the S-N curve, thus the two approaches to modeling fatigue are interrelated. The S-N curve, developed from full-scale test data, has built into it some initial and final crack lengths. If these crack sizes can be accurately characterized, the Paris Law allows them to be explicitly included in the analysis. Note that the exponent of 3 in the Paris law is the same as the inverse slope of the S-N curves. All S-N curves in the design codes, such as AASHTO, AWS, BS7608, DnV, and ABS Safehull [5] use a constant inverse slope of 3.

Fatigue tests are often described by their applied stress intensity factor range, or load ratio. The load ratio, or R-ratio, is expressed as:

$$R = \frac{s_{min}}{s_{max}} = \frac{K_{min}}{K_{max}} \qquad \text{Eqn. 0-6}$$

where σ_{max} and σ_{min} are applied stresses, and K_{max} and K_{min} are applied stress intensity factors. By convention, tensile stresses are positive.

Several definitions of ΔK exist which characterize the effectiveness of a loading cycle on crack growth. When tensile loading is applied, plasticity forms in the region surrounding the crack. This region has been stretched to occupy more area than previously occupied by the same material. Upon removing the tensile load, the plastic region remains permanently deformed, creating compressive forces around the plastic zone when the surrounding region unloads elastically. As the crack grows, a plastic zone path is left in the wake of the crack. These plastic zones can be seen in Figure 2-4.

Elber [45] theorized that this wake, and the compressive forces ahead of the current plastic zone, has the tendency to keep the crack closed under limited amounts of applied tension. This phenomenon is known as crack closure. A crack will only grow when it is opened fully at the tip. Therefore, a portion of the tensile loading may not contribute to new crack growth and only serves to open the crack.

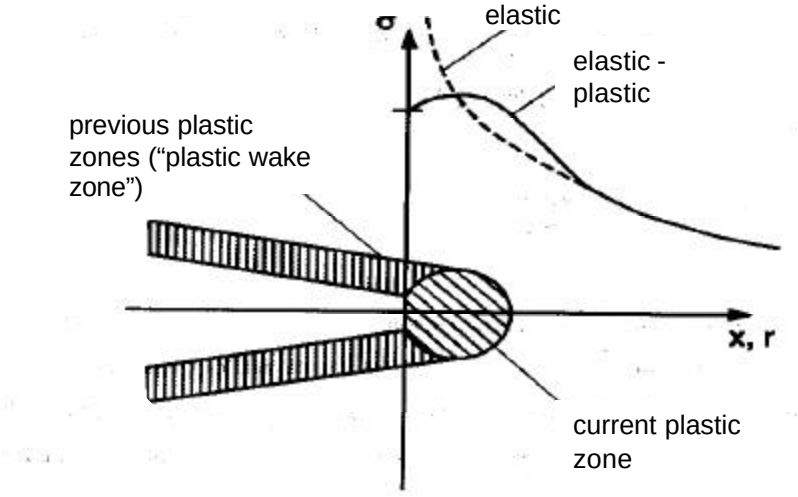

Figure 2-4. Plastic zones formed in crack growth [109].

Elber defined the effective tensile loading as:

$$\Delta s_{eff} = s_{max} - s_{op} \qquad \text{Eqn. 0-7}$$

where σ_{op} represents the amount of load necessary to open the crack up to the tip.

A ratio describing the effectiveness of an applied cycle was also defined:

$$U = \frac{\Delta s_{eff}}{\Delta s} = \frac{s_{max} - s_{op}}{s_{max} - s_{min}} = \frac{\Delta K_{eff}}{\Delta K_{applied}} \qquad \text{Eqn. 0-8}$$

where $\Delta K_{eff} = K_{max} - K_{op}$

K_{op} is defined as the amount of stress intensity factor necessary for the crack front to open. This includes all the effects of internal forces—namely, that of residual stress and plasticity effects. De Koning has presented an approach when plasticity effects are to be considered [88]. In the case of most fatigue crack growth, however, plasticity effects are assumed to be negligible because the majority of fatigue cycling occurs at stresses well below the material yield stress. The effective stress intensity factor for opening the crack can be determined by the procedure outlined in Figure 0-5.

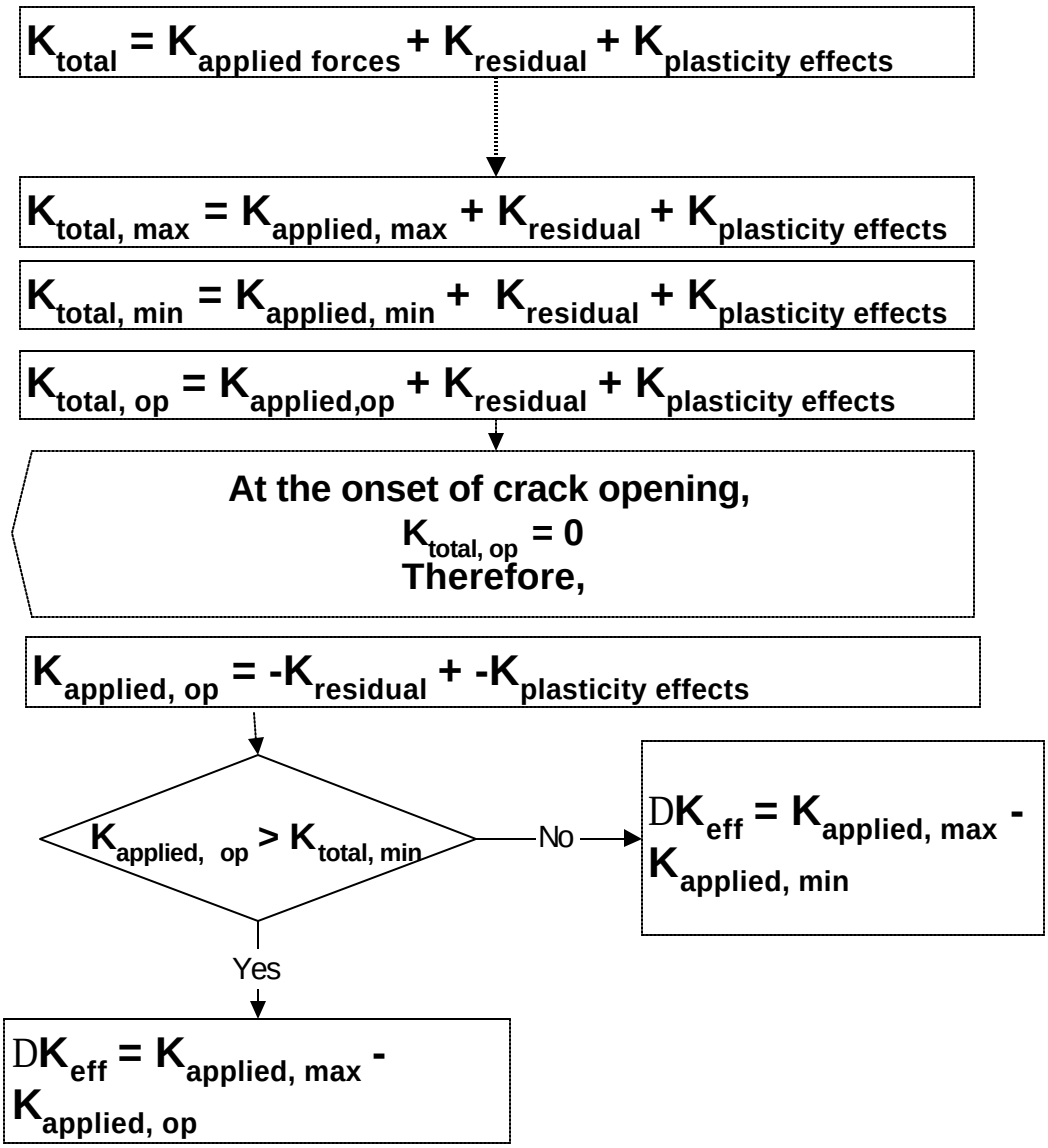

Figure 0-5: Procedure for determining effective stress intensity factor range [109].

In regions of compressive residual stress (for which the K-factor solution will be discussed later), K_{op} can be quite large and possibly consume most of the applied stress intensity factor. When the effective stress intensity factor is low, crack growth may slow down. If the effective ΔK decreases below the ΔK_{eff} threshold, the crack will arrest. Definitions of these various stress intensity factor ranges can be seen graphically in Figure 2-6.

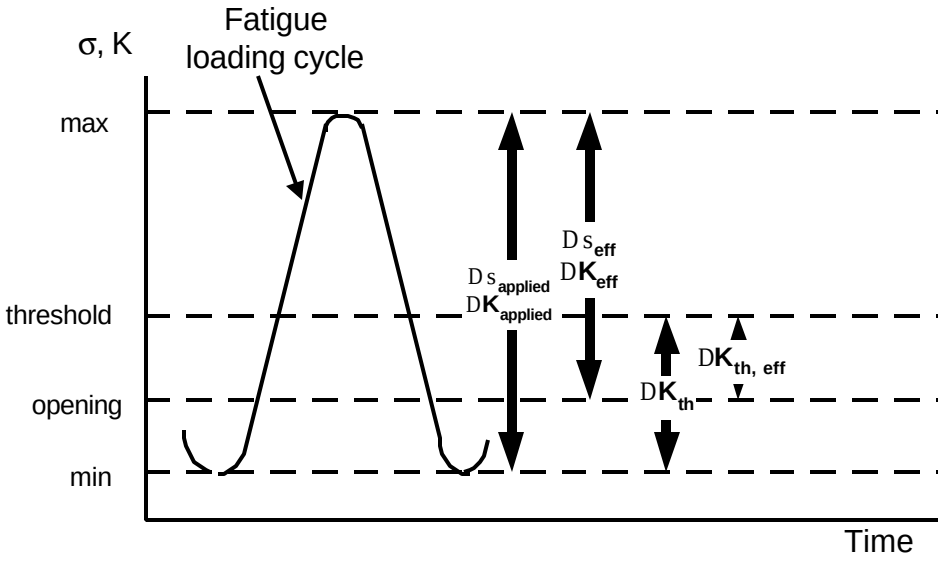

Figure 2-6: Definitions of K-factor ranges.

A great number of references are available to discuss the Paris Law and various modifications suggested to account for factors such as residual stress [22, 6]. A comprehensive guide to fatigue crack growth can be found in Ellyin's recent work [46].

2.2 SHIP DESIGN AND ASSESSMENT GUIDELINES FOR FATIGUE AND FRACTURE

Many papers have addressed the problem of cracking and crack propagation in ship structures, giving guidelines on a wide range of issues from design to maintenance to repair. A good overview of fatigue crack growth in ship structure is presented by Francis et al. [58]. The Ship Structure Committee has published a series of reports addressing various aspects of design, maintenance and assessment [43, 80, 81, 99, 100, 128, 130]. Specifically, SSC-244 established toughness requirements for ship structural steel. Minimum toughness requirements were specified in terms of both the 5/8-inch ductile tear test and Charpy V-notch test.

Prof. Stanley T. Rolfe of the University of Kansas significantly influenced the SSC-224 report. His 1974 paper [128] summarized the application of fracture mechanics to ship hull design and fracture performance. Rolfe identified the key factors to insure ductile failure modes, and discussed the interaction among them. Primary factors in crack growth were the stress level, flaw size and material toughness, while secondary factors included temperature, residual stress and loading rate. To assure ductile behavior, a minimum value of 339 Joules was recommended based on the 16-mm ductile tear test conducted at room temperature. A coupled criterion was that the ratio of the fracture toughness to the yield stress was at least 1.5, where fracture toughness is in units of ksi-in$^{1/2}$ and yield stress is in ksi. (Fracture toughness to yield strength ratio must be greater than 0.24, where fracture toughness is measured in MPa-m$^{1/2}$ and the yield stress in MPa.) These conditions were considered conservative because they were based on the assumption of dynamic loading in the ships, while in reality the loading rate is tending toward static more so than dynamic.

Specific ship structural steels were studied in 1973 by Kinoshita et al. in Japan [85]. Large plate specimens of mild and high strength steel were tested, verifying that their fatigue behavior could be predicted using the Paris Law. In addition, a ship hull corner detail with an edge notch was tested and modeled with finite element analysis (FEA). Both a constant amplitude loading and a two-step

loading was performed, the results of which suggested the Paris Law in conjunction with FEA K-values could be successfully applied to ship hull crack propagation.

Jordan et al. [80, 81] documented fatigue sensitive details in older ship structures. Cracking in tanker ships is documented in a series of reports from the Tanker Structure Cooperative Forum [149-151].

In 1993, Rolfe et al. directly addressed the high incidence of cracking in TAPS trade tankers [129]. Critical details were identified, where the ratholes near master butt welds and drainage holes presented the most critical concern. A characteristic material fracture toughness was determined from typical TAPS service tankers in terms of CTOD, with minimum values found in the base metal of .061 mm (.024 in). This toughness value was converted to an approximate value of K using the LEFM relation:

$$K_{Ic} = \sqrt{m d_c s_{FL} E} = 101.6 \cdot MPa\sqrt{m} \qquad \text{Eqn. 0-9}$$

where K_{Ic} = critical stress intensity factor, MPa*$m^{1/2}$

$m \approx 1.7$ based on research studies of structural grade steels

δ_c = CTOD value in m., in base metal of TAPS trade tankers = $6.1x10^{-5}$ m

E = modulus of elasticity, $206.9x10^3$ (MPa)

σ_{FL} = flow stress (Average of yield and ultimate tensile strength), MPa

$$\frac{379\,MPa + 586\,MPa}{2} = 482.5MPa$$

This results in a K_{IC} value of:

$$K_{Ic} = \sqrt{1.7(6.1x10^{-5}\,m)(482.5MPa)(206.9x10^{3})}$$

$$K_{Ic} = 101.6 \cdot MPa\sqrt{m} = 92.5 \cdot Irwins$$

This value was rounded up to 110 MPa-$m^{1/2}$ to obtain a reasonable estimate of the critical crack size. Using LEFM, Rolfe calculated a critical crack size for the material based on the stress intensity factor for the through-thickness crack in an infinite plate under uniform tension. A

coefficient of 0.6 was used to account for the crack opening constraint, or crack growth retardation, provided by several stiffeners. The final relation is as follows:

$$K_{Ic} = (RF_{MS})s_{\max}\sqrt{pa_{CR}} \qquad \text{Eqn. 0-10}$$

where a_{CR} = Critical crack size half length, in m.

RF_{MS}= Reduction factor for multiple stiffeners, approximately 0.6

σ_{MAX} = Maximum working stress, given as $2/3\sigma_{ys}$ = 234.4 MPa

Solving for the critical crack size,

$$2a_{CR} = \frac{2}{p}\left(\frac{K_{Ic}}{0.6s_{MAX}}\right)$$

$$2a_{CR} = \frac{2}{p}\left(\frac{109.9MPa}{0.6x234.4MPa}\right) \approx 0.38 \cdot meters = 15 \cdot inches \qquad \text{Eqn. 0-11}$$

This LEFM approach is very conservative despite the omission of residual stress effects on crack growth, since an applied stress of 234 MPa would induce significant plasticity at the crack tip. Plasticity at the crack tip is not accounted for in an LEFM analysis, which treats the ductile steel as a brittle material. (Note LEFM *can* be applied to fatigue crack growth, however, because the vast majority of fatigue crack propagation occurs at applied stresses well below the yield stress of the material, thereby creating only a negligible amount of plasticity at the crack tip).

Rolfe's paper [129] went further to outline a method for extrapolating constant stress fatigue life predictions to variable amplitude loading. In concluding, it was recommended that a two year inspection interval could be deemed appropriate if cracks no larger than a 50-mm surface crack were allowed. If a 75-mm crack was to be the maximum allowed, then the recommended inspection interval was reduced to one year. Finally, it was noted that the actual reduction factor due to multiple stiffeners may be even lower than 0.6, although residual stresses were not taken into account, and suggested experimental determination of the actual effects.

Rolfe's calculation for a critical stress-intensity factor conservatively underestimates the critical crack size, based on service observations, i.e. cracks up to 8-m in length reported without

catastrophic fracture as indicated in the introduction. In SSC-393 [35], Dexter and Gentilcore illustrated that ships constructed with the minimum toughness materials would fail by net section collapse, in most cases, rather than brittle fracture. Garwood et al. [61] have corroborated this phenomena, outlining the assessment procedure provided by BSI PD6493 for structural collapse. However, Bacci and Ligaro [12] assert that brittle fracture can occur in any material given the right conditions. They present an evaluation procedure illustrating the transition between brittle fracture and ductile fracture.

The toughness of weld metal usually exceeds the base metal toughness, allowing the crack to propagate in a stable manner in most cases. In the heat-affected zone (HAZ) adjacent to the weld, many steels develop local brittle zones which may induce limited brittle fracture or "pop-in" fracture. Pisarski and Slatcher [121] have noted that these pop-in fractures will be limited in structurally redundant systems. Peak loading conditions, minimum design temperature and flaw location in the most brittle portion of the HAZ would need to be coincident for an extensive fracture to occur. In addition, these local fractures usually propagate into the higher toughness base metal where they are arrested.

2.3 FATIGUE CRACK PROPAGATION IN STIFFENED PANELS

A great amount of research has been performed in the past on the solution for the stress intensity factor for cracked, stiffened panels. Much of the research addresses crack growth in aircraft, and appropriately the studies are made on aluminum materials with either riveted or adhesive connections. These types of attachments limit crack growth in that a crack progressing in a shell will not propagate up into the stiffener. This presents the beneficial effect of load shedding, as the load originally placed on both the shell plate and the stiffeners is transferred to the intact stiffeners. In such a case, the crack may only grow to a limited length because the intact stiffeners constrain the crack opening displacement, thereby removing the driving force of the crack. The development of fracture mechanics analysis of stiffened panels sought to explain this behavior quantitatively.

As early as 1959, Sanders studied the case of an integral stiffener centrally located on a thin, orthotropic sheet with a symmetric transverse crack [135]. He made the simplification that the sheet was extendible only in the longitudinal direction, giving a solution independent of Poisson's ratio. Grief and Sanders [64] later revisited this assumption in 1965, developing a plane stress solution as well as the solution for a non-symmetric crack case. Arin continued the study to multiple stiffeners [8]. Isida [74] studied the effect of bending stresses in this problem in 1970, but for most stiffened plates in ships the effect can be neglected. Isida later developed a solution for a center-cracked panel with stiffened edges, once again incorporating the effects of bending stresses [76].

As mentioned previously, the driving force in fracture research of stiffened panels was their use in aircraft. Consequently, much research was devoted toward developing stress-intensity factor solutions for riveted, stiffened panels. Bloom and Sanders [21] first modeled the effect of a riveted stiffener on the stress intensity factor for both a symmetric and non-symmetric crack in 1966. Cartwright et al. [26] adapted the riveted stringer methodology to Dugdale's strip yield model [44] in 1978.

Mansoor Ghassem [62] developed the fracture diagram as a design aid to stiffened panels in 1980. The fracture diagram is a plot of the transition between brittle fracture and gross section yield, using LEFM to evaluate the stress intensity factor. An extension was made for crack tip plasticity by manipulating Dugdale's strip yield model [44] into a stress intensity factor. The fracture diagram assumed stable crack growth occurred up to the line denoting the failure surface. Furthermore, a computer code was written as a means of predicting the number of cycles to failure based on LEFM analytical K solutions. The concept seems to have merit, although the assumptions within the development of the computer code necessitate further study in stiffened panel application. Also, the approach did not take into account residual stresses and was compared to a limited amount of test data for stiffened panels.

In 1971, Poe studied fatigue crack growth rates in aluminum panels with both riveted and integral stiffeners [122-23]. He used the Paris Law in conjunction with LEFM stress intensity factors to predict fatigue crack growth. Crack growth predictions were backed by full scale testing of aluminum stiffened panels with varied rivet spacing and stiffening ratios.

In order to predict the crack growth rate according to the Paris Law, a stress intensity factor range is required to characterize the crack driving force. Closed form solutions for stress intensity factors for different loading conditions and geometries have been developed for years [104, 145, 131]. Poe combined the known solutions for a center through-thickness crack with remote, uniformly applied stress, symmetric point forces, and crack face pressure distributions. This procedure, known as superposition, was also demonstrated by Vlieger in 1973 [164].

Superposition, as well as LEFM, is valid only in cases of linear elastic behavior. However, since the vast majority of service stresses are well below the yield strength of the material, these principles may be applied to fatigue crack propagation. An illustration of his use of superposition in the case of riveted stiffeners is shown in Figure 2-7.

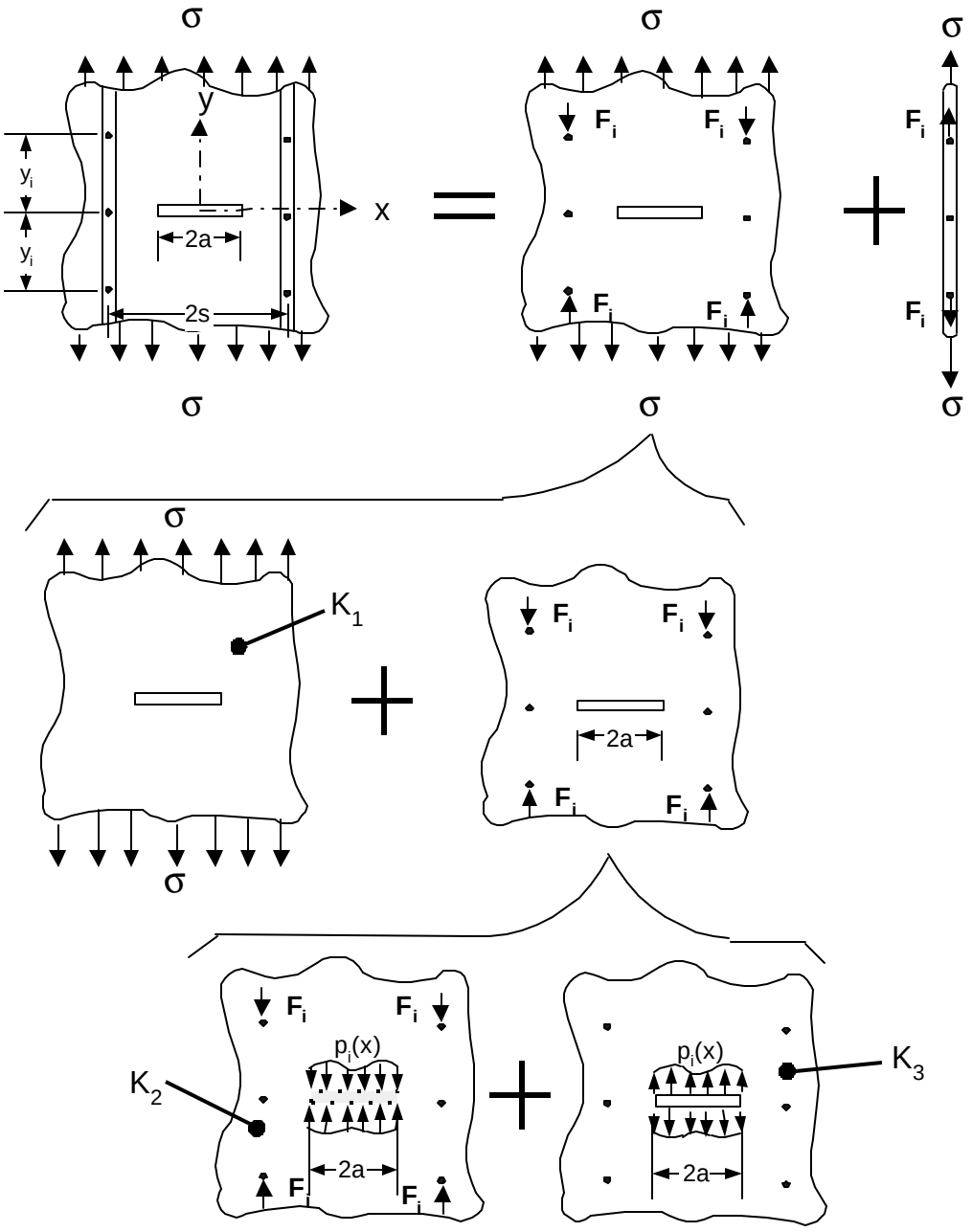

Figure 2-7: Use of superposition to develop analytical solution total stress intensity factor.

The stress intensity factor for the case of a plate with riveted stringers will now be explained. The stiffened panel can be subdivided into several contributions. First, the geometry is separated into two parts:

1. A plate subjected to uniform axial stress and stiffener connection forces
2. A separate stringer with reaction forces

The stiffener with reaction forces serves only as a means to determine the connection forces and does not contribute to the total K-factor. The connection forces are determined through displacement compatibility and force equilibrium between the stiffener and the plate, and the interested reader is referred to Poe's original work for the methodology (The connection forces will be determined through another means in this paper, as developed by Nussbaumer [109]).

Next, the plate is subdivided into two components:

1. A plate subjected to uniform axial stress, for which Equation 2-1 applies. For convenience, this relation is repeated here:

$$K_1 = s\sqrt{p\,a}$$

2. A cracked plate with connection forces, F_i, applied. This problem can be further broken down to two contributions:

A. An uncracked plate with a connection forces acting on it. If a crack *were* introduced, the crack faces must be free of shear and normal stresses. Therefore, a pressure distribution resulting from the connection forces is determined along fictitious crack faces, as shown. Since this component has no crack in it, the K-factor is zero ($K_2 = 0$)

B. An equal and opposite set of pressure forces must be exerted on the introduced crack. This distribution opposes the pressure distribution created by the connection forces and fulfills equilibrium, creating the stress-free condition along the crack faces. The stress intensity factor for a pressure distribution along the crack faces is:

$$K_3 = \sum F_i K_i = \sum \left[-F_i \sqrt{pa}\,\frac{2}{p} \int_0^a \frac{p_i(x)}{\sqrt{a^2 - x^2}}\,dx \right] \qquad \text{Eqn. 0-12}$$

where F_i is the contribution from the i^{th} set of symmetric rivets, and $p_i(x)$ is the pressure distribution determined using an i^{th} set of unit rivet forces.

The final result is assembled into a total expression for the stress intensity factor:

$$K_{Total} = K_1 + K_2 + K_3 \qquad \text{Eqn. 0-13}$$

The total stress intensity factor is often lumped into a single coefficient to be applied to the solution for the through-thickness crack in a plate subjected to tension. That is, a multiplier is developed as a function of the stringer and its connection:

$$K_{S.P.} = F(x, l, m)\sqrt{p\,a} \qquad \text{Eqn. 0-14}$$

where: ξ represents the rivet spacing ratio, d/2s

λ represents the transverse stiffener spacing ratio, a/2s

μ represents the stiffness ratio of the stiffener to the plate,

$$m = \frac{A_{st}E_{st}}{A_{st}E_{st} + (2s)E_{pl}} \qquad \text{Eqn. 0-15}$$

Decreasing the rivet spacing to a very small distance simulates the effect of having an integral stiffener. The crack may propagate into an integral stiffener and completely sever it. To develop the stress intensity factor, the K-factor was determined for various crack lengths. When the crack is near a stiffener (Around 0.95 times the stiffener spacing), the stiffener is considered completely severed and its load is shed to the remaining net section. Using this procedure, an abrupt jump in the K-factor is noticed due to the immediate loss of the stiffener.

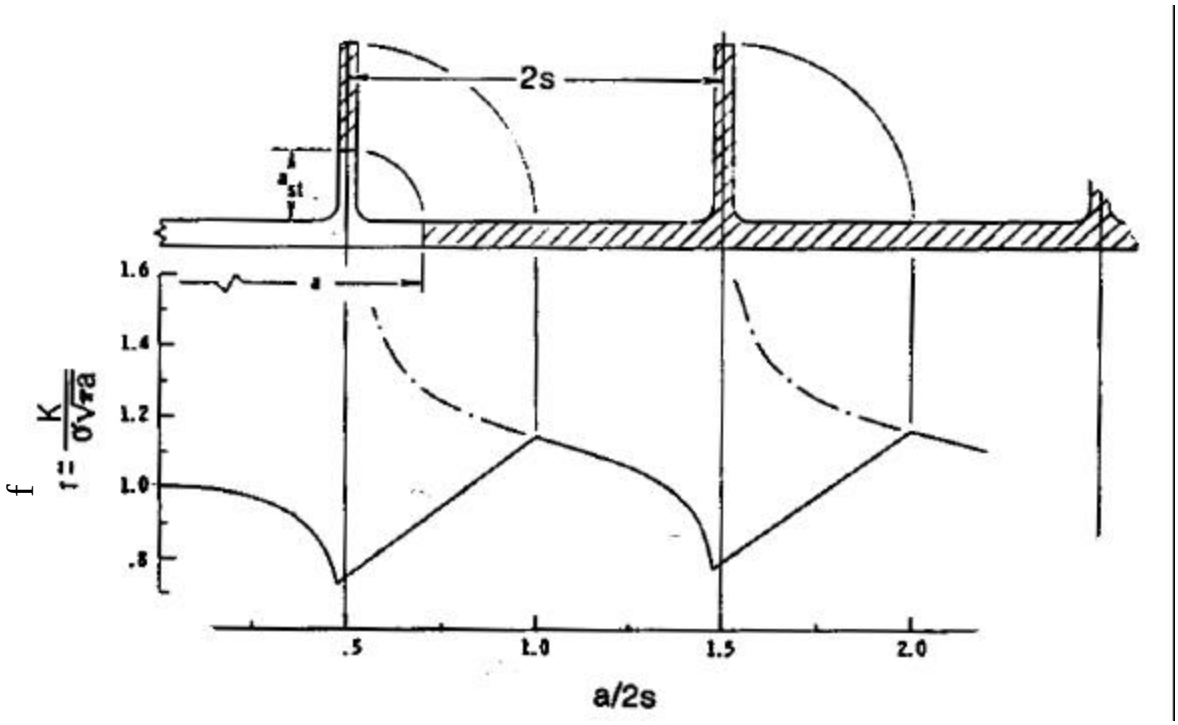

Figure 2-8: K-factor normalized to infinite plate solution in a panel with integral stiffeners [123].

Poe noticed that the crack grew at approximately the same rate in the stiffener as it did in the plate, which enabled a linear interpolation of the stress intensity factor between the solution for an intact stiffener and the completely severed stiffener. Figure 2-8 shows the results for the stress intensity factor as a function of crack length.

The resulting stress intensity factors could now be utilized in a fatigue crack propagation analysis. Comparing with experimental behavior, the predictions made using the resultant stress intensity factor with the Paris Law showed good agreement. Additionally, the relationship between stiffness ratio and cracking behavior could be directly forecast. Residual stresses, however, were not considered in the study.

Salvetti and Del Puglia conducted a similar study and approach on 6 different riveted stiffener configurations [134]. They studied 60 panels, under various constant amplitude loading conditions,

and noted discrepancies between Paris Law behavior and experimental behavior at different crack lengths.

Swift later modified Poe's solution for the case of flexible rivets [122] and adhesive panels [70]. Ratwani [71] studied panels with reinforcement attached through adhesion, comparing experimental stress intensity factors with both mathematical and finite element analysis results, including the effects of out-of-plane bending. Arin [8] studied the effects of plate orthotropy in adhesive stiffened panels on the stress intensity factor. He found little variation from that of an isotropic plate with stiffener, validating the initial assumptions made by Sanders in 1959.

Most of the aforementioned studies have been made on aluminum panels, often with riveted or adhesive bond stiffeners. In fact, there has been very little experimentation on welded, stiffened steel panels to determine fatigue crack growth rates. Kinoshita et al. [51] studied the Paris Law applicability to ship structural plate steel in 1973. His findings showed that the Paris Law effectively modeled crack growth in both typical ship structural plate and accurately described crack growth in a ship corner model.

The earliest work most closely fitting the current project's objective was performed by Watanabe et al. in 1979 [166]. The researchers studied crack propagation in a welded, stiffened panel typical of ship structures. Analytical modeling approximated the stress intensity factors for crack growth in the panel with stiffeners, using the Paris Law to evaluate the growth rate. Watanabe found that the predictions compared reasonably well with the actual behavior, although the extent of the investigation was limited to one configuration. The investigation, although limited in scope, demonstrated the possibility of using the Paris law in conjunction with LEFM to compute relatively accurate fatigue crack growth rates.

Petershagen and Fricke [120] conducted several fatigue crack growth experiments on stiffened panels. Experimental testing was emphasized in the study, although the effects of residual stress were neglected. Since much of the fatigue crack growth in ships occurs at low stresses, where

residual stress plays an important role, their inclusion is deemed necessary to correctly predict fatigue crack growth behavior.

Nussbaumer, Dexter, and Fisher [109-11] took residual stresses into account in a study on crack propagation through large-scale experiments on welded box girders. The experiments incorporated several fatigue sensitive details into a three-flanged box beam (See Figure 2-9), an attempt to simulate the structural redundancy found in unidirectional doubled-hulled ship structures.

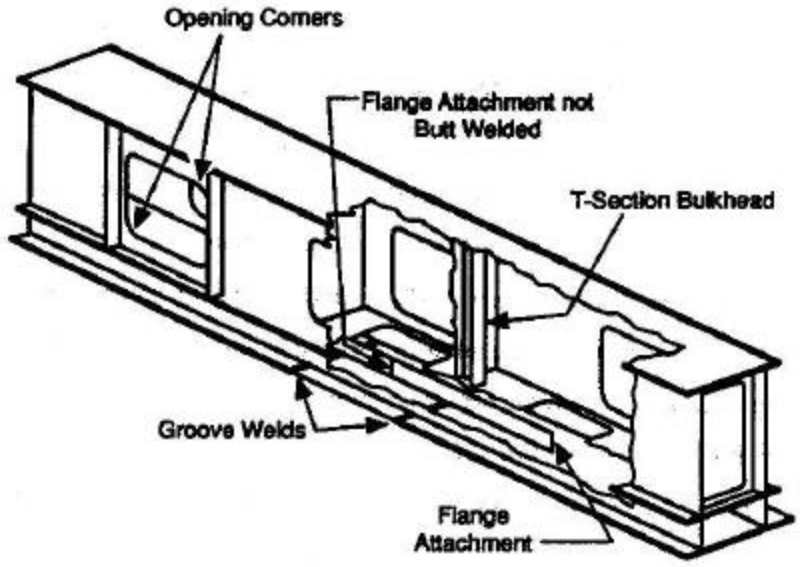

Figure 2-9: Test configuration and details investigated by Nussbaumer [109].

The present research will follow the objectives and methodology of Nussbaumer's work. The present research will extend the research of Nussbaumer et al. to the case of multiple stiffener plate geometry rather than the unstiffened cellular geometry.

Nussbaumer developed both an analytical and finite element models to address fatigue crack propagation based on LEFM. For fatigue crack growth, it was assumed that stresses significantly less than the yield strength of the material comprise the overwhelming majority of fatigue crack growth. Limited amounts of plasticity occur at these service stresses, allowing the principles of superposition and a simplified LEFM stress-intensity factor calculation to be used.

His analytical solution used the basic solution for a center crack in an infinite plate with a series of correction coefficients derived from the work of Isida, Poe, and Grief and Sanders [64, 74-76, 122, 123]. While Poe's work superimposed K-factors from applied loads (uniform axial stress and rivet point forces from stiffener-plate interaction), Nussbaumer's analytical model built upon Poe's model with the addition of a residual stress K-factor. The residual stresses were modeled based on Greene's function, integrating the solution for a pair of splitting forces acting at the crack faces. The K-factor due to residual stress is as follows:

$$K_{RES} = \sqrt{p\,a}\,\frac{2}{p}\int_0^a \frac{s_{RES}(x)}{\sqrt{a^2 - x^2}}\,dx \qquad \text{Eqn. 0-16}$$

An illustration of the derivation can be seen in Figure 2-10. Graphically, the solution for a pair of splitting forces is transformed into an integrated solution for a uniform stress acting

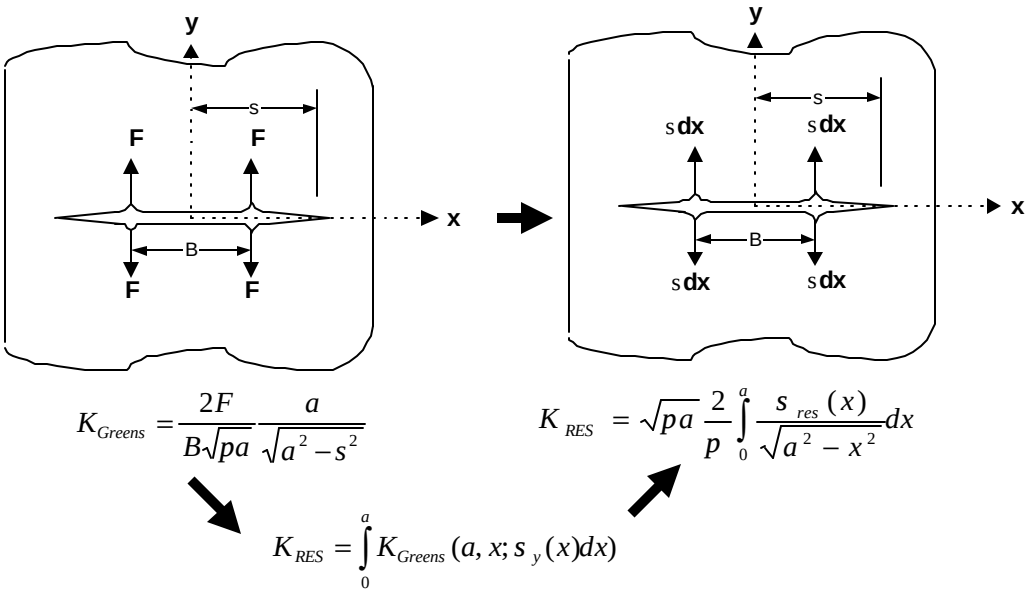

Figure 2-10: Use of Green's function to develop the stress intensity factor due to the residual stress field [131].

over an area, *dx*. Below the illustration, the accompanying solution for a pair of splitting forces (Left expression) is transformed into an integration of stress over an area, dx (Bottom, middle expression). Algebraic manipulation yields the resultant equation for a stress field acting on the crack face over an area *dx* (Right expression).

The LEFM K-factor solutions used were all developed for infinite plates subjected to various loads. Several coefficients have been used to correct for the finite width of the plate, but these tend toward infinity as the plate becomes fully cracked.

Nussbaumer proposed a net section coefficient to account for the finite width effect. The net section may be defined as the full cross section of the ship less the cracked components, cutouts, and holes. Cracking a stiffened plate in a redundant structure has the effect of increasing net section stresses. In other words, the stiffness of the structure may be expressed as a function of crack length. Such a correction would more adequately simulate the finite width effect than other suggested coefficients. Referencing the initial geometry of the structure, the increase in net section stresses can be determined from the net section modulus:

$$f_s = \frac{s}{s_{nom}} = \frac{I_0 c(a)}{I(a) c_0} \qquad \text{Eqn. 0-17}$$

where: I_0 = original moment of inertia

c_0 = original centroid

I(a) = Net section moment of inertia

c(a) = Net section centroid

Nussbaumer's [109-111] finite element model (FEM) consisted of determining J-integral at various crack lengths and translated it to an equivalent K. The J-integral is determined by taking a contour integral around the crack tip. It is a measure of the change in potential energy associated with extending the crack an infinitesimal amount, *da*. Many commercial finite element packages are equipped to perform such a calculation.

Before applying any external loading to the finite element model, residual stresses were input as applied temperatures causing shrinkage. An iterative process was employed on the *uncracked* geometry to develop the stress patterns measured in the specimens. A crack was then introduced, i.e. releasing boundary conditions along the nodes defining the crack faces, and the finite element

analysis automatically redistributed the residual stresses by maintaining force equilibrium. Use of contact elements along the crack face prevented overlapping of surfaces. These residual stress patterns redistribute as the crack propagates since they are originally configured on the uncracked geometry. This procedure will be followed in the current study, and a more detailed procedure will be discussed later.

When the stress intensity factor range is based only on the applied stress range (no residual stresses), both the analytical model and the FEM model predict increasing growth rates. Residual stresses were then considered in these models. A typical distribution of residual stress in a stiffened panel structure is shown as compared to the experimental data in Figure 2-11.

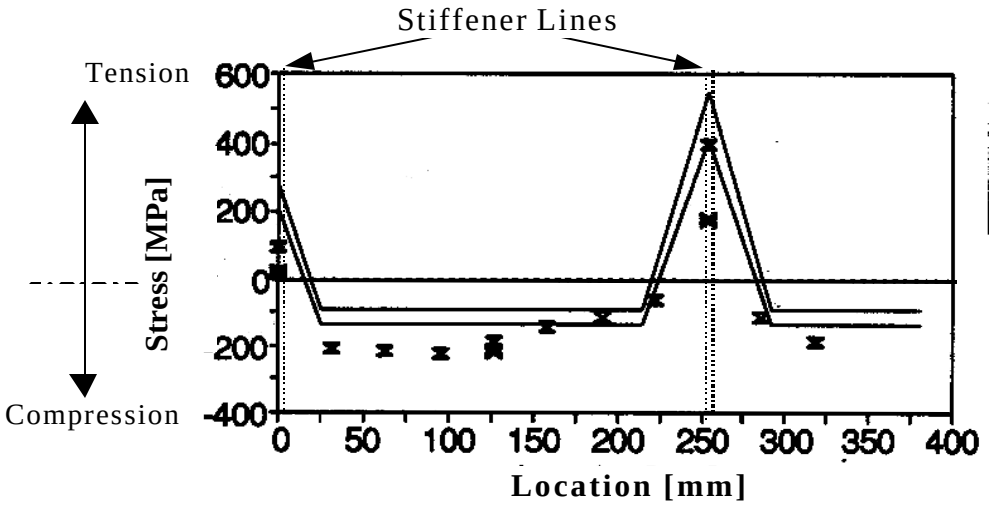

Figure 2-11: Typical residual stress field at fillet welded joints—used in Nussbaumer's analytical model [109-111].

There was significant scatter in the measured residual stress distributions for these experiments. Therefore, three distributions were examined, one based on the lowest observed residual stresses, one based on the largest observed residual stresses, and one that was an average or typical distribution. All of the distributions were in self-equilibrium,that is, compression zone area was equated by the area of tensile zones throughout the entire box section.

All three residual stress distributions were applied to the FEM model. The average distribution gave results that were generally just below the experimental data in terms of the growth rate. The maximum residual stress distribution causes a dramatic decrease in the growth rates to the point of virtual crack arrest. The minimum residual stress distribution gave results that were good up to 100 mm of crack length but then were too high in growth rate. These results show that the calculations are extremely sensitive to the residual stress within the range of variation that was observed.

In fact many other variables, including the difference between the upper bound growth rate and the lower bound growth rate, made minimal difference in the calculations in comparison to the residual stress. Therefore, if modeling of this type of crack propagation is to be improved, it is not necessary to know the crack growth rate (above threshold) any more accurately, and more effort should be focused on studies of the residual stress and how it is affected by fabrication sequence. Better data on the threshold crack growth rates would improve modeling of the first stage of crack growth, however.

In the analytical model, the average residual stress distribution was used directly in its corresponding K-factor, K_{RES}, Eqn. 2-16. The residual stresses were not redistributed as the crack propagated. Such redistribution, although factual, was deemed too complicated to incorporate into the analytical model. Only the tensile part of the stress intensity factor range was considered effective and was used in the Paris law (The effective stress intensity factor is defined in Figure 0-5).

Based on the effective stress-intensity factor range, the analytical model gave reasonable results, as compared to the experimental data in Figure 2-12. The finite element model, where K-factors are determined through converted J-integrals, and residual stresses were redistributed, provided similar results.

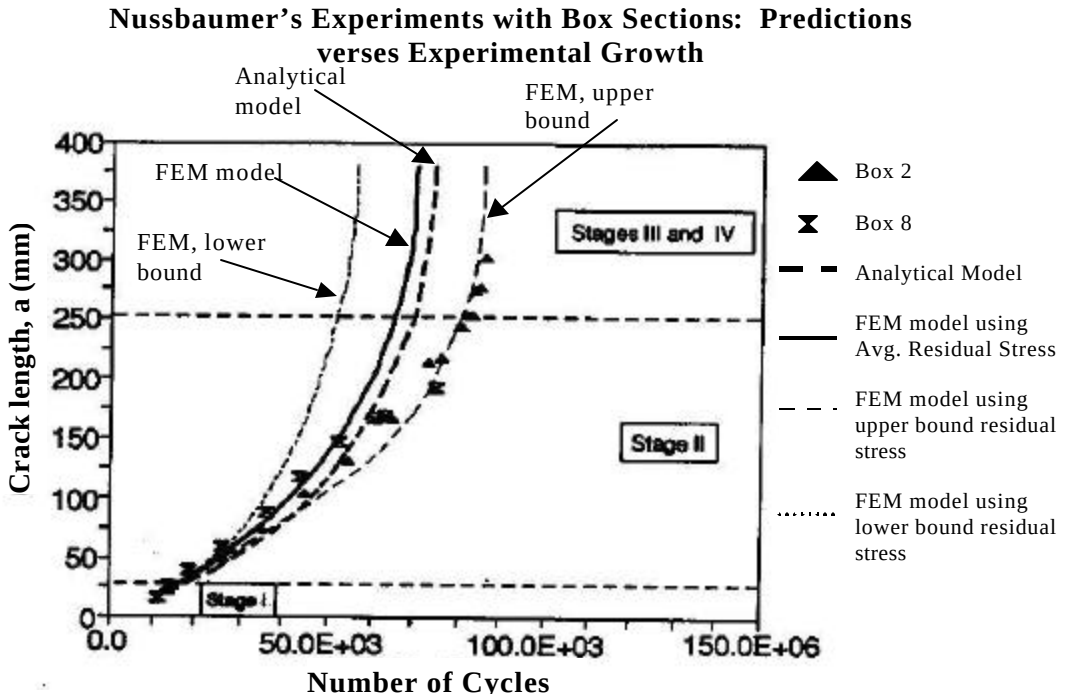

Figure 2-12: Fatigue crack predictions for cellular box beam [109-111].

Nussbaumer found that both the analytical model and the finite-element (FEM) model predicted the behavior reasonably well in the one-celled box beam (See Figure 2-12), and that neglecting the effect of residual stresses increased the error significantly. In addition, the FEM model predicted crack closure at and behind the crack tip, consistent with the observations. In an extension of his research, Nussbaumer analyzed a multi-cellular box structure representative of a ½ scale model of a double-hulled vessel. His FEM predictions indicated that the crack opening stress was significant in accurately modeling the crack growth, due to crack closure effects. With the multi-celled structure, the crack opening stress was predicted through finite element analysis. The analytical model, however, is not capable of accurately predicting crack closure effects. However, no experimental data were available for comparison.

It is noteworthy that in the box girder tests, unless the cracks were repaired, they continued to propagate in a stable manner until it was impossible to load the specimens due to excessive

deflection. The cracks often reached more than 1.5 meters in length, giving a clear demonstration of the inherent structural integrity of a cellular structure fabricated from relatively thin plate (13 mm or less) of reasonably tough steel.

Several other investigators have used techniques similar to Nussbaumer's models. A decade before Nussbaumer, Anil Thayamballi's Ph.D. dissertation [154] outlines an almost identical analytical approach to calculating fatigue crack growth through stiffened panels, including the effects of residual stress. In addition, variable amplitude loading, ship failure assessment and residual strength of ship structure are discussed. The residual stress distribution was determined using the representative block tension and compression regions suggested by Faulkner [48-50], with the same integrated Green's function as used by Nussbaumer. The dissertation includes an exhaustive reference section of works pertinent to assessing fatigue crack growth, ship structural failure, and wave loading representation. However, no experimental verification was made to verify the approach and its assumptions.

In 1996, Sumi et al. [142] used finite element analysis to study fatigue crack propagation in stiffened panels similar to the deck structure in ship. A single crack in a stiffened panel and an array of three cracks initiated at the stiffener locations was investigated, neglecting the effects of residual stress. Equivalent K-values were computed using ANSYS finite element software. Four specimens were tested: A plate with a center crack, a plate with an array of three cracks, and a stiffened panel with a single crack, and a stiffened panel with an array of three cracks. The applied stress range was 80 MPa, and the initial crack length was 8 mm in all cases.

The research was similar to the present course of study except for the exclusion of residual stress. LEFM ΔK values were used in the Paris Law to predict crack propagation rates in mild steel. For the case of multiple cracks, a simple iterative solution was developed hinging on a reference crack. The predicted results for the plate specimens were reasonably accurate, while the predictions for the stiffened specimens over-estimated the fatigue life by about 25 percent. The authors attributed the error to lack of residual stress inclusion, noting the behavior in the stiffened specimens with respect to their predictions.

Other researchers using the analytical, LEFM-based approach to fatigue life prediction include Pang in 1991 [116] and Cook et al. in 1992 [29]. Pang explored surface fatigue cracks emanating from both welded cruciform joints and fillet shoulder. His analytical analysis of surface crack propagation used a material threshold stress intensity factor to account for crack closure. This work, however, did not attempt to account for residual stress, and the prediction errors (some being highly conservative) was attributed to the uncertainty in the material threshold.

Cook et al. [29] outline a computer program developed to address cracks propagating from rivet holes in aircraft structures. Although the program addresses fatigue crack growth in aluminum panels with riveted stiffeners, it includes the effects of residual stress at holes with compressive residual stress introduced through cold expansion techniques. Cold expansion, along with interference-fit connections, has become a common technique to increase fatigue resistance at rivet holes in damage tolerant design. A LEFM superposition approach similar to Thayamballi's [154] was used to incorporate a stress intensity factor due to residual stress. The residual stress field, however, was characterized more precisely by Lagrangian interpolation rather than the simple linear interpolation illustrated in Figure 2-9. Stress intensity factors were determined through the use of Green's function, with a resulting expression similar to Equation 2-17. Fitzpatrick and Edwards provide an overview of this technique and its relation to residual stress fields [56]. Essentially this is a means of determining K-values for a specific configuration through weight functions, where 8^{th} order Guassian integration was used to accumulate the total stress intensity factor for a varying stress field.

Cook's approach, although more detailed in determining stress intensity factors, did not resolve the shortcomings of Nussbaumer's analytical model. Namely, the residual stress field was not redistributed with crack growth, and crack closure behind the crack tip was not taken into account. Therefore, the main enhancement of this model was the refined characterization of residual stress field and its subsequent integration. These corrections may be appropriate for application to cold expansion residual stresses, where the stress fields can be characterized with relative accuracy.

Welding residual stresses, however, vary so significantly that a refined approximation cannot be justified at this time and a linear, worst-case model is more applicable.

To date, the previously mentioned works were the most significant advances in this subject. Many authors have confirmed the strong influence of residual stress on crack growth, although very little experimentation has been conducted in long fatigue crack growth. The subject of residual stress and its affects on small-scale fatigue and fracture has been studied extensively, however. A review of its role in fracture and plastic collapse is presented by Clayton [27].

1.5 RESIDUAL STRESS

Residual stresses in welded steel structures can contribute to the problems of: 1) hydrogen-assisted cracking during fabrication; 2) brittle fracture during fabrication or in service; or 3) fatigue crack growth in service. Therefore, it is important to be able to predict the magnitude and distribution of residual stress. A good overview of residual stress effects on fatigue and the complexities involved in predicting fatigue crack growth through residual stress fields is provided by Fitzpatrick and Edwards [56]. An excellent work on residual stresses and their effects in ship hulls can be found in an early book by Osgood [114].

Residual stress has a profound effect on fatigue, but it does not need to be taken onto account explicitly in fatigue design or evaluation using S-N curves. This is because the S-N curves are already adjusted to reflect the worst-case effect of residual stress. S-N curves are a lower bound to a large sample of large-scale tests with the natural residual stress distributions in the welded specimens. Thus, the appropriate worst-case level of residual stress is built into the S-N curves. The high tensile residual stress in welded details means that the mean level of applied stress has little impact on the fatigue life, which also simplifies fatigue design and evaluation procedure.

There are special situations where residual stress should be explicitly considered in fatigue evaluation using a crack propagation analysis. For example, it is necessary to know the residual stress distribution for the analysis of long propagating through-thickness cracks beyond the initial fatigue life given by the S-N curves. It is assumed that there are high tensile residual stresses in the vicinity of the stiffener-to-plate welds. Therefore, it is only necessary to know the compressive part of the residual stress distribution that is far away from the weld. Therefore, complex models to predict the residual stress are really not necessary for this application. Simplified methods, typically idealized representations of residual stress fields based on experimental data, remain the best option for routine engineering assessment.

The uncertainty in the additional life due to long crack propagation is dominated by the uncertainty in the residual stress. Variations in the expected residual stress are due to the initial residual stress in the plates and rolled shapes prior to welding, thermal cutting, and fabrication sequence. Plates and members are straightened at the mill to conform with tolerances. After fabrication, assemblies may be flame straightened to correct plate out-of-flatness or weld distortion. The resulting uncertainty can change the crack propagation rate by more than two orders of magnitude. Narrowing this uncertainty will have the greatest payoff in terms of increased confidence in structural integrity.

Fracture is very sensitive to microstructure and significant benefits could be obtained by continuing to study how the weld thermal cycle affects fracture toughness. Ductile fracture is not affected by residual stress [57], however brittle fracture is dramatically affected by residual stress. This is only an issue in evaluating existing structures, because new structures should not be designed using brittle materials.

Typically, worst-case assumptions are made regarding the residual stress in brittle fracture evaluations. In fact, this simplifies the evaluations significantly because the peak stresses (applied plus residual) are taken as equal to the actual yield strength. This eliminates the need for determining the applied stresses. In rare cases, it is acceptable to take into account some reduced residual stress other than the worst-case assumption. However, it dangerous to narrow the margin too much on the possibility of brittle fracture. This is the only situation where a detailed description of the residual stress, such as could be obtained with a numerical simulation, would be useful for fatigue and fracture design or evaluation.

A large amount of measured residual stress data from rolled shapes and welded built-up members have been obtained over the years at Lehigh, primarily by Lambert Tall and his colleagues [4, 19, 86, 147, 153]. Experimental data [4, 19, 53, 60, 86, 147, 153] show that the initial residual stress in welded and rolled sections is highly variable and depends on the fabrication process. The ranges in the value of peak tensile residual stress are at least plus or minus 40% about the mean.

Another significant factor that must be taken into account is fabrication sequence. Measured residual stresses in box sections depend strongly on which web is welded to the flange first [53, 115]. When there is excess gap between members to be welded, they are often pulled together using a "come along", which has a profound effect on the built in residual stress in many neighboring members. Flame straightening may be used to correct plate out-of-flatness or weld distortion, which also alters residual stresses.

Many of these issues were faced through compression research of stiffened panels [48-50, 71, 72, 87, 105,124,139, 165]. Vroman took residual stress data in 3 identical steel stiffened sheet panels in 1995 [165]. The configuration was typical of naval vessel structures, and is seen in the Figure 2-13.

The specimens were fabricated at the Naval Surface Warfare Center (NSWC) at Carderock, Maryland, with the welding sequence being typical of naval ship construction. Measurements were taken throughout the fabrication process through use of a Whitmore gage: Once prior to welding, once after tack-welding the stiffeners to the plate, and finally after welding was completed. The data points were spaced at 70 mm in the center bay only, with results for the three panels as indicated in Figure 2-14.

Normally one would expect high tensile regions around the stiffener region, with equilibrating compressive stresses in between stiffeners. The measured forces across the panel do not satisfy equilibrium, and thus the data must be questioned. It is likely that the measurement spacing did not accurately capture the narrow tensile regions surrounding the

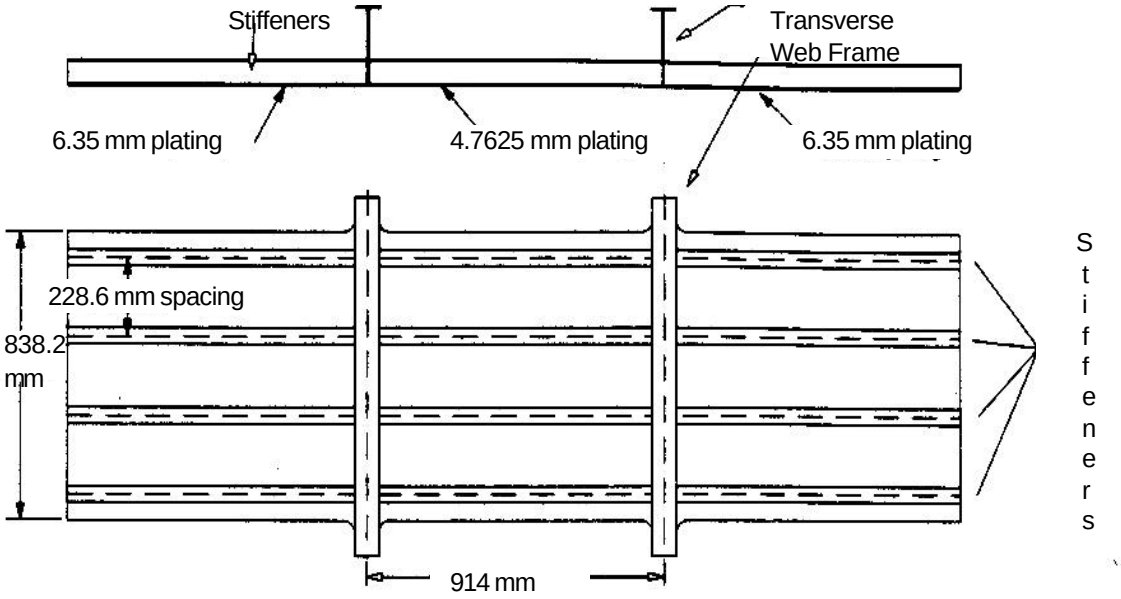

Figure 2-13: Typical grillage tested by Vroman [165].

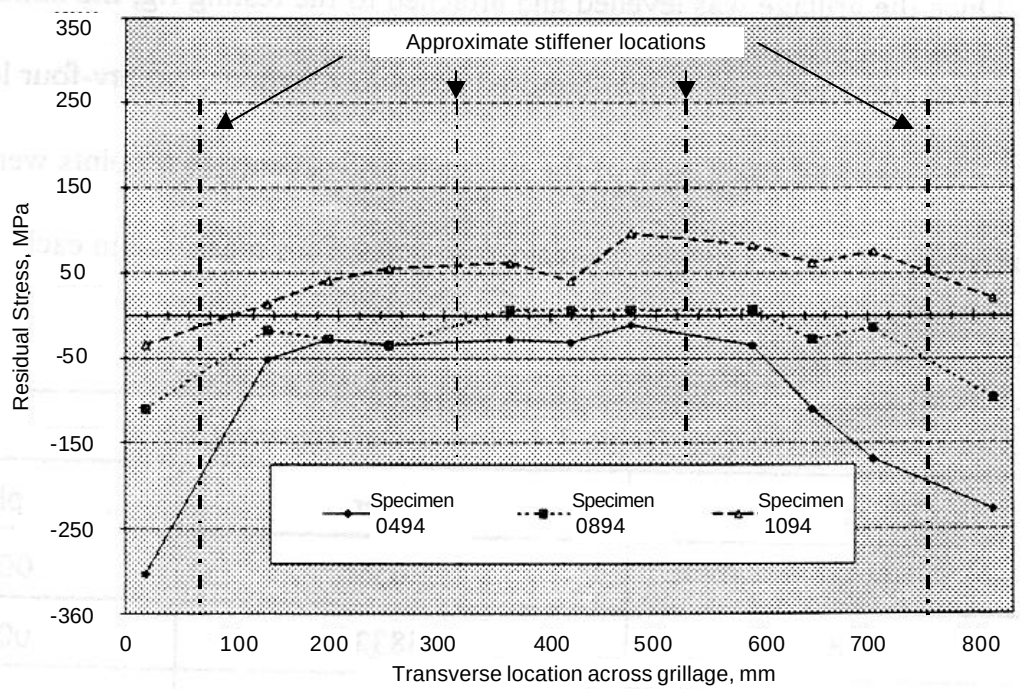

Figure 2-14: Residual stresses in three stiffened panels tested by Vroman [165].

stiffeners. An important note in Figure 2-14 is the variation in measured residual stresses despite the fact that the steel plating was "carefully selected from a large batch to all exhibit similar strengths, mean stresses, etc." In fact, yield stress measurements in the stiffeners were all matched at 383 MPa, the plating matched at 305 MPa, and the welding pattern unchanged. Even with such rigorous quality control, the difference between the residual stress data in the three identical panels is apparent.

Earlier compression tests by Kondo and Ostapenko provide a more accurate profile of the residual stress field. Their sectioning coupon pattern was more refined (See Figure 2-15).

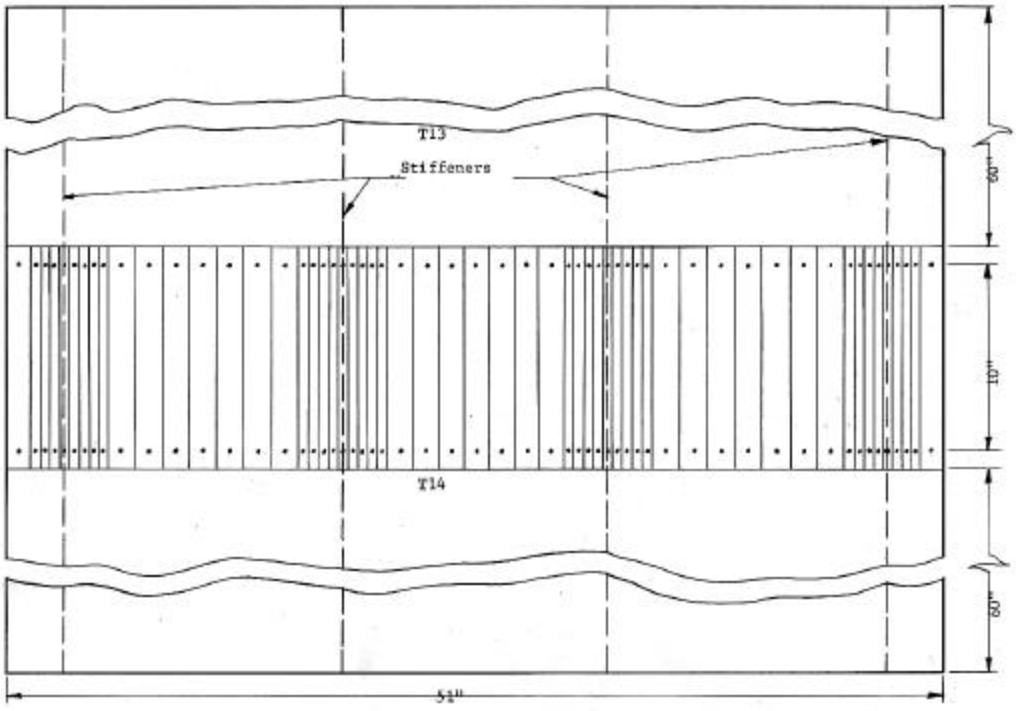

Figure 2-15: Coupon pattern used in sectioning of tested stiffened panels by Kondo and Ostapenko [102].

This fine sectioning pattern was carefully measured and extracted to obtain residual stress measurements. The results may be seen in Figure 2-16. This plot characterizes the residual stress pattern expected in welded stiffened panels. The measurements capture the tensile zones around the stiffener weld lines and demonstrate the equilibrium conditions found in residual stress patterns.

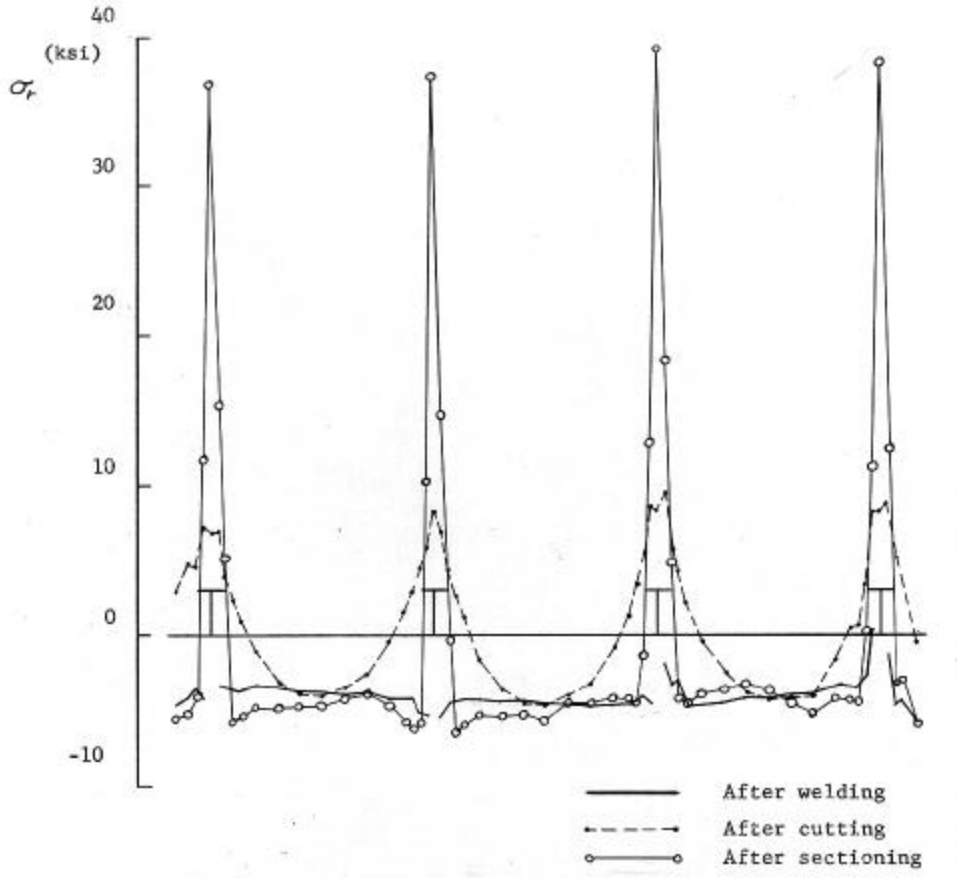

Figure 2-16: Residual stress measurements obtained by Kondo and Ostapenko [102].

Compression tests at Simon Engineering Laboratories at the University of Manchester [71, 105], and at Monash University in Australia [105], included measurements of residual stress. Totaling over 40 tests, the results provide residual stress data for a variety of welding configurations on various stiffener geometries. In particular, a large number of hole-drilling measurements were taken across some panels with geometry similar to the current investigation's configuration, with the exception of a smaller weld size (6-mm). As typical, there was a wide range of residual stress measurements in very similar panels.

Notwithstanding this uncertainty, welding simulation models have been developed and have been used for some practical applications [7, 39-42, 63, 67, 83, 95, 96, 132, 133, 160-162]. Kamtekar [83] provides a review of the development of residual stress prediction attempts. He demonstrated

an iterative procedure using the finite difference method to predict residual stress patterns. Significant simplifications are typically used to make the numerical analyses feasible. For example, two-dimensional generalized plane-strain models have been used in most cases. Despite the simplifications, these analyses are far from routine. Yet there is a need to model complex three-dimensional connections. Such three-dimensional calculations require significant labor to set up and significant resources to run. For these reasons, numerical welding simulation has remained primarily a research tool rather than a part of routine engineering assessment of fracture critical structures.

Simplified methods, typically idealized representations of residual stress fields based on experimental data, remain the best option for routine engineering assessment. The simplest method of analysis is to rely on measurements in a similar hot-rolled or welded built-up structural member. Tall and Alpsten [147] state that peak longitudinal residual stresses in hot-rolled and built-up structural members can be estimated within 70 MPa based on experimental data and empirical rules.

The typical residual stress distribution for stiffened panels and box sections was shown in Figure 2-11. This idealized distribution is based on the work of Faulkner [48-50], who stated that the width of the tensile zone, assumed to be at a stress equal to the yield strength, is equal to between 4 and 5 times the thickness of the panel, independent of stiffener spacing. The net tensile force is balanced with a region of constant compression between the stiffeners. In addition, the following formula was given by Faulkner et al. [50] for characterizing the residual stress field between stiffeners:

$$\frac{s_r}{s_o} = \frac{2h}{\left(\frac{b}{t}\right) - 2h} \qquad \text{Eqn. 0-18}$$

where η = coefficient for determining the width of the tension block, ηt

σ_r = magnitude of the compressive residual stress block

σ_o = yield stress of the plate

b = stiffener spacing

t = plate thickness

Typical values for η in as-welded ships range from 4.5–6, while values of 3–4.5 were given to account for the shakedown of residual stress in ship service. This equation assumes an idealized situation in which both the compressive and tension zones are rectangular blocks. Modeling the tensile block as a triangular region (Figure 2-11) gave the empirical residual stress distribution used by Nussbaumer, Dexter and Fisher [109-111], a distribution confirmed to be relatively accurate in recent experiments on box sections [115]. This type of residual stress distribution should be used for cracks in the shell of ship structure propagating between stiffeners.

For more complicated geometries, a simple estimation of peak values of residual stress can often be obtained by considering a uniaxial elasto-plastic model. The strain can be estimated with the average coefficient of thermal expansion and the difference between the phase transformation temperature and room temperature. This strain is applied to the uniaxial model to estimate the peak stress [95]. This approach does not give the distribution of residual stresses through the thickness of the plate.

In order to estimate the distribution of the residual stresses, the actual multiaxial behavior of the component must be considered. If simple analytical models exist for the component (e.g. a simple beam or plate), the tendon-force or shrinkage-force approaches [17, 20, 93, 94 146, 167] may be used. In these approaches a force is calculated and applied to the component along the weld axis, in a way similar to that of a prestressing tendon. The reaction of the component to this force gives the residual stress. In the simpler applications, this force is taken as 20% of the heat input [94, 167] or proportional to the weld area [17, 20]. The more sophisticated approaches consider the temperature distribution in the weld and are usually attributed to Russian papers by Okerbloom [57].

There are simple numerical models, for example Tall [146], which generally break the plate or other geometry into fibers or strips. The transient temperature distribution is applied and strain compatibility is enforced among the strips. These models are generally applicable to only a specific type of component. The finite-element method offers greater flexibility and accuracy. The justification for the strip models is the savings in computer time relative to advanced nonlinear

transient finite-element analyses. Since modern computers are increasingly able to handle these finite-element analyses, there is no longer any reason to consider the strip models.

An example of finite element analysis to determine residual stress distributions is shown by Finch and Burdekin [51]. They illustrated the residual stress field in a butt welded plate and a butt welded pipe-on-plate geometry, and calculated J-integrals for various crack lengths and loads. Interestingly, they found [for the butt welded plate] that the J-integral obtained in a plate with residual stresses was always larger than that of a plate without residual stress, even when the crack was well into the compressive region. Furthermore, they found that at certain loads, the plate with a small crack in the tensile region of residual stress had a higher J-integral than the case where the crack had penetrated the compressive region. The plate with the small crack, therefore, would have the non-intuitive aspect of being more susceptible to cracking than the plate with the larger crack in the compressive residual stress zone.

This behavior of crack propagation was also noted by Almer et al. [3]. A series of experiments was performed on compact specimens with and without residual stress introduced. A similar study was conducted by Bucci [24]. X-ray diffraction was used to quantitatively measure the residual stress field and compared to finite element analysis. The finite element analyses compared relatively well with the x-ray diffraction measurements with the exception of overestimating the residual stress near the source of tensile residual stress. The researchers noted that crack propagation rates became highly sensitive to residual stress as the applied loading decreased. Such behavior reinforces the importance of characterizing worst-case residual stress patterns, especially in ship loading conditions where many of the applied loads are very small.

The beneficial effects of compression zones on crack propagation have been noted for quite some time. Many investigators have sought means of exploiting the compressive regions as crack arresters through a process called “stress coining”. An analysis and discussion has been conducted by Ogeman et al. [112] on the applicability of this process to longitudinal connections at web-frame intersections.

Averbach and Lou [11] noted the crack propagation rates in carburized compact specimens. Using superposition, they defined an internal stress intensity factor to account for the residual stress according to a distance, d_i, correlating with the extent of residual stress, and δ_i, the residual stress at a given point. Their simple relation was as follows:

$$K_i = d_i d_i^{\frac{1}{2}} \qquad \text{Eqn. 0-19}$$

This relation was added to the applied stress intensity factor to determine the effective stress-intensity factor, K_e.

Beghini et al. [16] studied the effects of residual stress in a series of compact specimen tests in 1994. They modified an expression from Tanaka [148] to account for the plasticity-induced crack closure, an attempt to approximate the effective stress intensity factor actually occurring at the crack tip. Weight functions were used to modify the stress intensity factor, and experiments indicated that the superposition of the residual stress K-factor was only applicable for cracks with no closure. The authors, however, remarked that crack closure would not have significant effects in the case of long cracks [16]. When comparing the predictions including residual stress with those that neglected residual stress, the results showed conclusively the important influence that residual stresses have.

Torii et al. [155,156] studied surface crack propagation through residual stress fields in 1989, indicating that the crack propagation rate could be based on a combination of the applied stress intensity factor and the maximum stress intensity factor. Their results modified the Paris Law into the form:

$$\frac{da}{dN} = C(\Delta K)^p (K_{max})^q \qquad \text{Eqn. 0-20}$$

where p and q were empirical coefficients that satisfied the relation: p + q = 1

Although the results were based on an elliptical surface flaw in a compact specimen, the approach provided a new formulation for the Paris Law that could hold significance.

Another modification of the Paris Law was presented by Toyosada et al. based on an effective ΔK called the ΔK_{RP} [157, 158]. The ΔK_{RP} parameter is defined as the stress intensity factor required to

overcome the effect of the previous plastic zone. When the crack is opened with significant applied loads, a plastic zone is generated around the crack tip, which tends to keep the crack tip closed. With the crack held closed by the plastic zone, part of the applied stress is not effective since a portion of the applied tension is devoted to overcoming the plasticity-induced closure.

The ΔK_{RP} takes into account the plastic deformation ahead of the crack tip that has occurred from previous load cycles. In regions of tensile residual stress, the ΔK_{RP} decreases, translating to more a more effective ΔK range and faster growth rate. In regions of compressive residual stress, the ΔK_{RP} increases, taking into account the beneficial effect of compressive residual stress maintaining the closed crack front.

The study was based on a modification of Newman's crack closure model [139], where plastic shrinkage along the crack faces and redistribution of the plastic zone ahead of the crack was taken into account. Compact experiments showed good agreement with the model, but the improvement of the predictions in tensile-only cycling was negligible. Its merit could be significant in variable amplitude loading where both compressive and tensile cycles exist, although the complexities involved in variable amplitude loading undermine the method's ease of use.

Itoh et al. [77] and Ohji et al. [113] have demonstrated that the use of a simpler LEFM ΔK_{eff} based on the crack opening load was sufficient to produce reasonable crack growth rate correlation. Neglecting the redistribution of residual stress was found to be conservative with positive R-ratios, and propagation rates were equivalent with respect to the crack opening ratio, *U* (Elber's ratio) [45]. For convenience, Elber's ratio is restated here:

$$U = \frac{\Delta \sigma_{eff}}{\Delta \sigma} = \frac{\sigma_{max} - \sigma_{opening}}{\sigma_{max} - \sigma_{min}} = \frac{\Delta K_{eff}}{\Delta K_{total}}$$

Itoh et al. programmed this approach into a computer, providing crack growth estimations relatively quickly. A flow chart for such an algorithm is presented in the paper as well.
This simplified approach seems prudent in light of the uncertainties involved. It is anticipated that such a procedure will be effective in providing worst-case estimates of crack growth, although the

accuracy in any one test may be compromised. Leggatt has confirmed this approach as satisfactory [92]. He comments on the application of the approach in PD6493 procedures and outlines the extension toward CTOD design curves and J-integral schemes, which are comparable to Xiao and Dexter's methodology [169] and the procedure followed by Stenseng [141].

1.6 VARIABLE AMPLITUDE LOADING AND STRUCTURAL RELIABILITY

So far, crack propagation has been discussed as if the loading were constant amplitude. However, the actual service load history of ships consists of cycles with a variety of different load ranges, i.e. variable-amplitude loading. Such wave loading data is found in SSC-268 [68]. Some attempts have been made to model crack growth behavior under a specified loading history [9, 14]. These models, often complex, generally address highly random flight loading and relatively simple models presented hereafter have demonstrated similar accuracy [10].

There are several accepted ways to convert variable stress ranges to an equivalent constant-amplitude stress range with the same number of cycles. SSC-315 addresses some of these methods, although comparisons were made with compact specimen testing [43]. These procedures are based on the damage summation rule jointly credited to Palmgren and Miner (referred to as Miner's rule [103]). Most large-scale experimental studies have confirmed the use of Miner's rule [137]. However, there is some experimental evidence that indicates that Miner's rule can be very conservative in some cases, and unconservative in others [162]. For more information on these effects, the interested reader can consult the work of Gurney [65], Solin [140], Engle [47], and Winter and Maccinnes [168].

The most rigorous way to calculate an equivalent constant-amplitude stress range with measured stress history data is to sort through the stress history in the time domain and count the stress ranges; i.e. specific differences between maximum stress peaks and minimum stress peaks. A stress-range occurrence histogram is then constructed from the cycle-count data. This procedure was analyzed by Thayamballi [154]. Other methods of calculating an equivalent constant-amplitude stress range

involve simple relations to statistical measures of the variability of the stress history such as the root-mean-square (rms).

For the cycle-counting approach, there are at least two widely accepted ways to count cycles: 1) the mean-crossing method; and, 2) the rainflow method. The mean-crossing method assumes that the stress-time history is essentially stationary about a mean value (for short periods) and a cycle is counted as the value of the stress passes from below to above the mean. The maximum and the minimum value of stress are the highest and lowest values that occurred in the time interval since the last mean crossing. Intermediate oscillations between successive mean crossings are ignored, counting only the one cycle with range equal to the maximum minus the minimum.

The rainflow method counts cycles as closed loops within a cycle counting period. Essentially, the largest maximum is matched with the largest minimum, then the second largest pair is matched, and so on. The rainflow method does count intermediate oscillations as individual cycles. One problem with rainflow counting is that, depending on how long the cycle-counting periods are, a maximum may not be associated with a minimum until numerous mean crossings have occurred. This seems inconsistent with the fact that a propagating fatigue crack could propagate beyond the location where the maximum occurs before the corresponding minimum occurs and the cycle is counted.

Another issue with cycle counting is a cutoff or threshold. Depending on the sampling frequency and the precision of the data, there will be very large numbers of very small oscillations. It is generally agreed that these very small oscillations do not have a significant effect on the fatigue life, so typically some arbitrary cutoff is used below which cycles are ignored. In practice, a cutoff of about 3.5 MPa is typically used.

Once the stress range occurrence histogram is developed, the equivalent constant-amplitude stress range can then be calculated using Miner's rule [103]. If the exponent of the S-N curve is equal to 3, then the relative "fatigue damage" of stress ranges is proportional to the cube of the stress range. Therefore, the effective stress range is equal to the cube root of the mean cube (rmc) of the stress ranges, i.e.:

$$S_{Re} = [\, S_i \, (n_i/N_{total}) \; S_i^{\,3} \,]^{1/3} \qquad \text{Eqn. 0-21}$$

where S_{Re} = effective constant-amplitude stress range,

n_i = the number of stress ranges in interval associated with S_I , and

N_{total} = the total number of stress ranges in the stress time history.

The ratio n_i / N_{total} is equal to the fraction of the total stress ranges in the interval of magnitude S_i.

As previously mentioned, there are some simple methods of estimating an equivalent constant-amplitude stress range directly from the statistics of the variability of the stress history. The root-mean-cube (rmc) stress range can be estimated indirectly from the rmc acceleration amplitude from ship motion studies. This approach relies upon a linear relation between the stress range and the acceleration that must be obtained from dynamic structural analysis or from correlation of measured data.

In previous work on fatigue of highway sign structures for the National Cooperative Highway Research Program, another simple approach was used [82]. The effective constant-amplitude stress range is assumed to be equal to 2.8 times the rms of the stress. In this case, the rms can be determined directly from power spectrum data. Note that this rms is the rms of the stress time history itself, not a property of the stress ranges, as is the rmc stress range described above. Therefore, there is no need to count cycles from the actual time histories when using these simple approaches.

An effective constant-amplitude stress range should be estimated for several discrete levels of Sea State. Then, using an estimate of the period from each sea-state such as the significant wave period, the number of cycles in each sea state can be estimated from the number of hours in each sea state.

The fraction of the life that is consumed by a certain duration of a specific sea state can be obtained from the ratio of the number of cycles in that duration to the number of cycles to failure (N_{total} from Miner's rule) for the effective constant-amplitude stress range associated with that sea state. If a

mission profile can be defined that consists of a series of sea-states, the total fraction of life consumed by that mission is the sum of the fractions consumed at each sea state. The total number of missions that can be carried out before failure is the reciprocal of this fraction of life per mission. A good example of this type of analysis can be found in a paper by Sikora et al. [137].

The plasticity at high levels of stress will have the effect of increasing crack closure and therefore reducing crack growth rate. Therefore, it is conservative to ignore this effect in the effective stress range concept. However, it is important to compute a unique effective stress range whenever the character of the loading changes significantly, e.g. as in a storm.

A number of authors have developed methods of fatigue failure assessment through probabilistic methods [10, 28, 59, 79, 82, 90, 139, 168]. A recent report [100] summarizes the state of the art in reliability analyses for ships. Since these methods are statistical analyses and the objectives of the current study focus on the determination of crack growth rate, only a brief summary will be presented.

Freudenthal and Shinozuka [59] considered upper and lower bounds of ship survival. They observed the scatter in fatigue life prediction of aluminum details and concluded that these lives were a random variable with respect to constant and variable loading. They formulated a statistical life-estimation model based on the multiple load path nature of a redundant structure comprised of many of these details.

Jiao [79] discussed a fatigue reliability model based on the Paris law in which the crack growth rate was considered a random variable except its dependence on crack size. This was assumed because of the variability in loading and its corresponding effect on crack size. Sequence effects are incorporated in a model developed by Columbi and Dolinski [28]. Lambrigger [90] provides a commentary on the use of Weibull probability distribution functions for assessing material failure, a commonly used approach for determining critical crack sizes. This approach is outlined by Alaa Mansour for computing peak wave loadings [101], and detailed in SSC-322. For an in-depth review, the reader is directed to the original works.

Soares and Garbatov [139] present a method based on the section modulus of the ship hull at any given point in time. They related a ship's reliability to the incidence of repair and inspection, and compared their methods with case studies of two tankers. The results showed intuitive conclusions—that increased inspection and repair highly contribute to the structural reliability of the hull at any given point.